

# **VIRTUAL SYNCHRONOUS MACHINE PHASE SYNCHRONIZATION**

by

**Joseph James Petti**

Bachelor of Science, University of Pittsburgh, 2016

Submitted to the Graduate Faculty of

The Swanson School of Engineering in partial fulfillment

of the requirements for the degree of

Master of Science

University of Pittsburgh

2018

UNIVERSITY OF PITTSBURGH  
SWANSON SCHOOL OF ENGINEERING

This thesis was presented

by

Joseph Petti

It was defended on

March 21, 2018

and approved by

Gregory F. Reed Ph.D., Professor, Department of Electrical and Computer Engineering

Zhi-Hong Mao Ph.D., Associate Professor, Department of Electrical and Computer Engineering

Brandon Grainger Ph.D., Assistant Professor, Department of Electrical and Computer Engineering

Thesis Advisor: Gregory F. Reed Ph.D., Professor, Department of Electrical and Computer  
Engineering

Copyright © by Joseph James Petti

2018

# **VIRTUAL SYNCHRONOUS MACHINE PHASE SYNCHRONIZATION**

Joseph Petti, M.S.

University of Pittsburgh, 2018

This thesis enables virtual synchronous machine (VSM) control by contributing resynchronization of phase among parallel-connected distributed generation (DG). The work presents simulation, modeling, and testing to demonstrate the benefits and liabilities that VSMs control offers in place of the conventional phase-locked loop (PLL). This investigation came to light due to the recent and impending increased penetration of power electronic based generation. As the grid modernizes, generation has shifted and will continue to shift from conventional power plants that operate large synchronous generators to power electronics-interfaced DG. This shift is due to environmental, financial, and sustainable goals set by the government, corporations, and individual citizens. Particularly renewable energy, such as solar and wind, have become popular replacements because of the availability of the resources. Both of these generation types pass through the control of power electronics when injecting power onto the grid.

PLLs have been the main tool used to synchronize power electronic sources to the grid they are operating within. They have proven to be an excellent tool for synchronization but in some situations this is also their downfall. They synchronize to the strongest source available and mimic the behavior of this source regardless of quality. As the distributed power electronic generation profile grows and the synchronous machine generation profile declines the grid will lose valuable inertia. This inertia is readily available today because of the large amount of synchronous generation still present. Inertia is used to sustain stable operation in the wake of grid disturbances, such as faults.

The grid will become less stable, as increased penetration of DG dissipates inertia. Virtual synchronous machines have become a solution to solve this issue, simultaneously allowing for mass penetration of renewable energy. The virtual synchronous machine is a power electronic converter control method that utilizes the swing equation, inherent to synchronous machines, instead of the conventional PLL, in order to be synchronous to the grid. Virtual synchronous machines mimic inertia, where synchronous machines inherently operate with inertia, and can aid grid stability in wake of grid disturbances.

As this power electronic based generation is added to the grid inertia can be lost. The VSM is a control strategy that gives power electronic based generation inertia, adding robustness to the grid. The VSM is very stout in the area of frequency stability but not in phase stability. This work aims to improve the VSM in order to give it better phase stability. This improvement will make VSMs a more useful tool in terms of stabilizing the grid.

## TABLE OF CONTENTS

<b>TITLE PAGE .....</b>	<b>I</b>
<b>COMMITTEE MEMBERSHIP PAGE.....</b>	<b>II</b>
<b>ABSTRACT.....</b>	<b>IV</b>
<b>TABLE OF CONTENTS .....</b>	<b>VI</b>
<b>LIST OF TABLES .....</b>	<b>X</b>
<b>LIST OF FIGURES .....</b>	<b>XI</b>
<b>PREFACE.....</b>	<b>XIII</b>
<b>1.0 INTRODUCTION.....</b>	<b>1</b>
<b>1.1 POWER GENERATION.....</b>	<b>2</b>
<b>1.2 CHALLENGES POSED BY GENERATION CHANGE TO THE MACROGRID .....</b>	<b>2</b>
<b>1.3 CHALLENGES POSED RENEWABLE ENERGY TO MICROGRIDS .....</b>	<b>5</b>
<b>2.0 BACKGROUND .....</b>	<b>6</b>
<b>2.1 DISTRIBUTED GENERATION .....</b>	<b>6</b>
<b>2.2 MICROGRIDS .....</b>	<b>7</b>
<b>2.3 VOLTAGE SOURCE CONVERTER.....</b>	<b>9</b>
<b>2.4 PHASE-LOCKED LOOP.....</b>	<b>12</b>
<b>2.5 VIRTUAL SYNCHRONOUS MACHINE .....</b>	<b>13</b>
<b>3.0 MICROGRIDS.....</b>	<b>15</b>
<b>3.1 TYPES .....</b>	<b>16</b>
<b>3.1.1 Urban .....</b>	<b>16</b>

3.1.2	Rural .....	16
3.1.3	Off-grid .....	16
3.2	DESIGN .....	17
3.2.1	Control .....	17
3.2.1.1	Four Main Hierarchical Control Levels .....	17
3.2.1.2	Centralized Vs. Decentralized Control .....	18
3.2.2	Protection .....	18
3.2.3	Generation .....	19
4.0	MICROGRID PROTECTION PROJECT .....	20
4.1	MICROGRID ISLANDING EXPERIMENTATION .....	20
4.1.1	IEC 61850 – GOOSE Protocol .....	21
4.1.2	Real Time Digital Simulation - Hardware-in-the-Loop Technology .....	22
4.1.3	Procedure .....	22
4.1.4	Results .....	24
4.1.5	Findings .....	26
4.1.6	Impact .....	27
5.0	VIRTUAL SYNCHRONOUS MACHINE MODELING .....	28
5.1	PHASE-LOCKED LOOPS .....	28
5.2	SWING EQUATION .....	29
5.2.1	Equation Variables .....	29
5.2.2	Examine Constants in the Equation .....	30
5.2.3	Constants Have a Large Impact on System Performance .....	31
6.0	VOLTAGE AND FREQUENCY ANALYSIS .....	34

6.1	TESTING PROCEDURE .....	34
6.2	TESTING CRITERIA.....	35
6.3	RESULTS .....	37
6.3.1	Conventional Phase-Locked Loop .....	37
6.3.2	Virtual Synchronous Machine.....	38
6.3.3	Parallel Combination of Conventional Phase-Locked Loop and Virtual Synchronous Machine.....	39
6.4	ANALYSIS .....	40
6.5	PERFORMANCE DISCUSSION .....	40
7.0	PROPOSED PHASE CORRECTION .....	41
7.1	TEST PROCEDURE.....	41
7.2	CONVENTIONAL PLL AND VIRTUAL SYNCHRONOUS MACHINE IN PARALLEL .....	42
7.2.1	Results.....	44
7.2.2	Analysis.....	46
7.3	PARALLEL VIRTUAL SYNCHRONOUS MACHINES .....	47
7.3.1	Results.....	49
7.3.2	Analysis.....	51
7.4	DIFFERENCES .....	51
7.5	CORRECTION.....	52
7.5.1	Grid Instability .....	52
7.5.2	Phase Angle Correction Algorithm Implementation .....	54
7.5.2.1	Testing Procedure .....	56



7.5.2.2	Results .....	56
7.5.2.3	Analysis .....	58
8.0	CONCLUSION.....	59
8.1	FUTURE WORK.....	59
	BIBLIOGRAPHY .....	61

## LIST OF TABLES

Table 1: Parameter values for VSC filter, VSM, and grid load .....	35
Table 2: Grid events and corresponding times .....	35
Table 3: Abnormal voltages .....	36
Table 4: Abnormal frequencies .....	36
Table 5: Synchronization frequency, voltage, and phase limits defined by IEEE-1547 .....	42
Table 6: Events and corresponding times .....	43
Table 7: Dp and J values for VSM1 and VSM2 .....	48
Table 8: Events and corresponding times .....	48

## LIST OF FIGURES

Figure 1. Traditional Vs. Modern Grid.....	2
Figure 2. Price of PV with and without tax credit .....	3
Figure 3. World Power Generation Projects .....	4
Figure 4. MG example .....	8
Figure 5. Voltage, current, frequency, and phase values extracted from the grid .....	10
Figure 6. PWM Diagram.....	10
Figure 7. Phase A reference signal Vs. Triangular wave.....	11
Figure 8. PWM signal that results from phase A reference signal Vs. Triangular wave.....	11
Figure 9. Schematic diagram of the conventional SRF-PLL.....	12
Figure 10. Swing Equation Control for an Inverter .....	14
Figure 11. Components of a MG .....	15
Figure 12. Oneline of grid connected MG .....	24
Figure 13. RTDS HIL set up.....	24
Figure 14. a) Measured time of fault occurrence b) Measured time of MG islanding .....	25
Figure 15. Voltage p.u. islanding results .....	26
Figure 16. Frequency islanding results .....	26
Figure 17. Swing equation altered for VSM control.....	30
Figure 18. Frequency results for $J=4$ and $D_p=100$ .....	32
Figure 19. Frequency results for $J=2$ and $D_p=100$ .....	32
Figure 20. Frequency results for $J=4$ and $D_p=200$ .....	33

Figure 21. Voltage response of a VSC controlled by a conventional PLL.....	37
Figure 22. Frequency response of a VSC controlled by a conventional PLL.....	37
Figure 23. Voltage response of a VSC controlled by a conventional PLL.....	38
Figure 24. Frequency response of a VSC controlled by a conventional PLL.....	38
Figure 25. Voltage response of parallel VSC controlled by a convention PLL and a VSM .....	39
Figure 26. Frequency response of parallel VSC controlled by convention PLL and VSM.....	39
Figure 27. Conventional PLL and VSM in parallel MG set up .....	43
Figure 28. Per unit power output of conventional PLL and VSM.....	44
Figure 29. Frequency results of the conventional PLL and VSM .....	45
Figure 30. Phase angle difference in degrees.....	45
Figure 31. Parallel VSM MG set up .....	48
Figure 32. Per unit power output parallel VSM.....	49
Figure 33. Frequency results of parallel VSMs .....	50
Figure 34. Phase angle difference in degrees.....	50
Figure 35. Phase angle difference between VSM1 and VSM2 .....	53
Figure 36. System voltage without phase angle correction algorithm.....	54
Figure 37. Swing Equation used to calculate $\omega_{VSM}$ and $\Theta_{VSM}$ .....	55
Figure 38. Modified Swing Equation.....	55
Figure 39. Per unit power output of VSM1 and VSM2.....	56
Figure 40. Frequency response of VSM1 and VSM2.....	57
Figure 41. Phase angle difference between VSM1 and VSM2 .....	57
Figure 42. MG load voltage .....	58

## **PREFACE**

There are a vast number of co-workers, friends, and family without whom the completion of this thesis would never have been possible. The support, input, and assistance I received from them was essential in the development and completion of the work that appears in this document.

I would first like to thank my mentor, Patrick Lewis. From the first week I started working in the graduate group to the last week, and into the future, Pat has been a teacher, motivator, guide and friend. The support he has given me cannot be given justice by any amount of words.

I would also like to thank the rest of my colleagues at the University of Pittsburgh's GRID Institute. These co-workers, or more accurately friends, helped me to strive towards my degree through their intellectual contribution, as well as their friendship and support. In no particular order, these fine engineers are: Dr. Katrina Kelly, Tom Cook, Alvaro Cardoza, Chris Scioscia, Zach Smith, Santino Graziani, Jake Friedrich, Thibaut Harzig, Matthieu Bertin, Sam Morello, Dr. Hashim Al-Hassan, and Dr. Ansel Barchowsky.

I would also like to thank my committee and advisors, Dr. Gregory Reed, Dr. Brandon Grainger, and Dr. Zhi-Hong Mao. Their advice, guidance, and technical support has been incredible. I am lucky to have walked in their footsteps and received the breadth of knowledge they relayed to me.

A special thanks is also owed to Transmission and Protection Engineering groups at Dominion Energy. In particular I am grateful to Kyle Thomas and Chris Mertz for mentoring me during my summer internship and fostering many of my engineering skills that allowed me to complete this process.

Another thank you is owed to my uncle, Frank Petraglia, for mentoring me since high school. Without his constant guidance and advice I do not know if I would have completed this process or even entered the field of engineering.

Finally, I would also like to thank my parents, Joe and Carol Petti, for being such incredibly positive influences in my life and for helping me to reach towards this goal. Their love and support has been amazing, and I could never have made it here without them.

## **1.0 INTRODUCTION**

The traditional electric power grid, Figure 1, used high voltage (HV) transmission system to connect large central generating stations to a distribution system that directly fed customer demand. Generating stations consisted primarily of fossil fuels and hydro based resources that created power via high inertia turbines [1]. Over time, technological advances have led to changes in the power grid. The modern grid, Figure 1, incorporates increased distributed generation (DG), renewable power sources, communication, electric vehicles, and more to create a more efficient and effective grid [1].

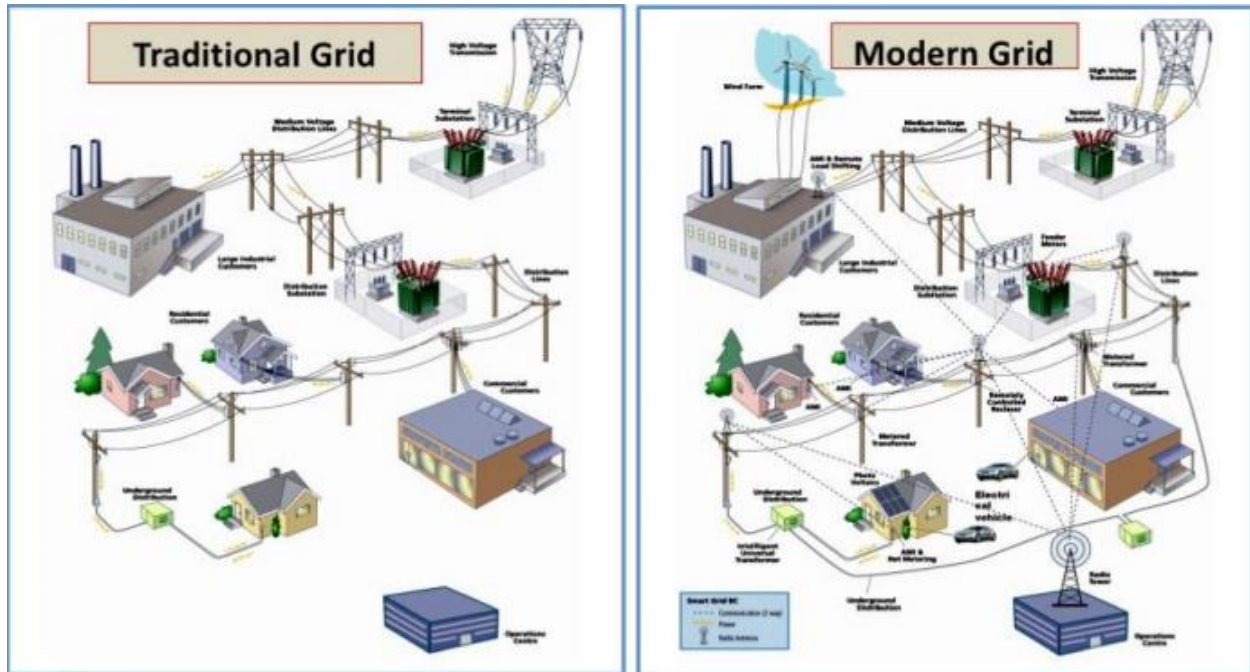


Figure 1. Traditional Vs. Modern Grid

## 1.1 POWER GENERATION

The days of large centralized generation dominating the power generation profile are numbered. DG is becoming more prevalent on the grid and will continue to become more so. DG offers the ability to increase efficiency and reliability of power systems [1] [2]. Of DG sources, renewables, wind and solar mainly, have become popular in spite of their high initial costs [3]. Future installations are more promising due to advancements in technology that will lower these prices and make renewable energy more efficient [3]. Figure 2 shows how solar-powered DG costs have lowered over time [3]. The cost is leveling out but at a rate that is favorable to utility customers trying to reduce consumption from the grid.



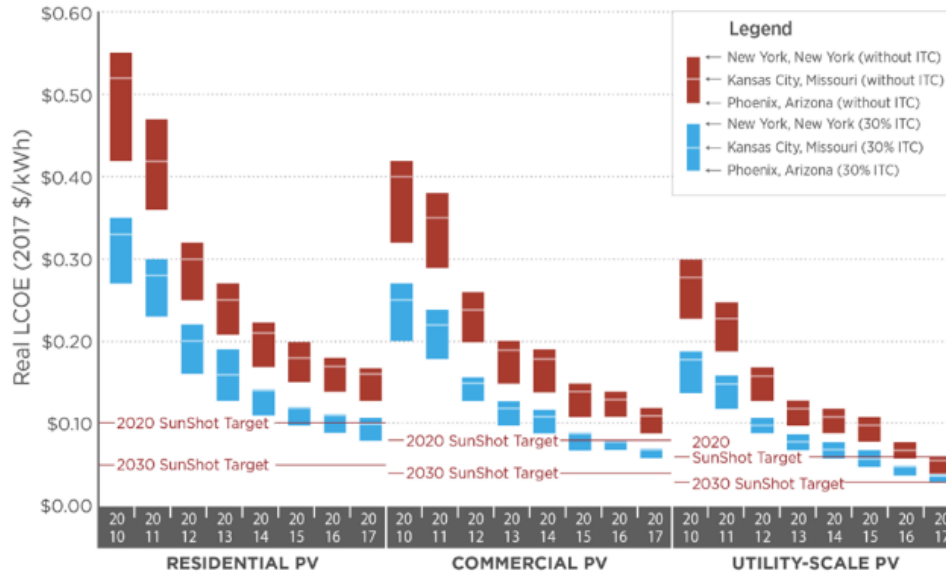


Figure 2. Price of PV with and without tax credit

Power electronics, inverters, and other converters, are needed in order to synchronize DG, particularly renewable sources, with the grid. The rigid synchronous machine (SM) is becoming less frequent as inverter-based design continues to rise in popularity due to the use of renewable energy and its flexibility. Figure 3 shows projections for many of the key electric power generation sources. Renewables are projected to have the largest increase over the next 35 years [4]. Conventional SM sources, such as coal and nuclear, are on the decline due to environmental and safety reasons, but natural gas is on the rise due to its low cost and low emissions [4]. The grid inertia, inherent to conventional SM generation and often taken for granted by many, is depleted as the penetration of inverter-based generation increases. As inertia dissipates, the grid will become more susceptible to stability issues [5].

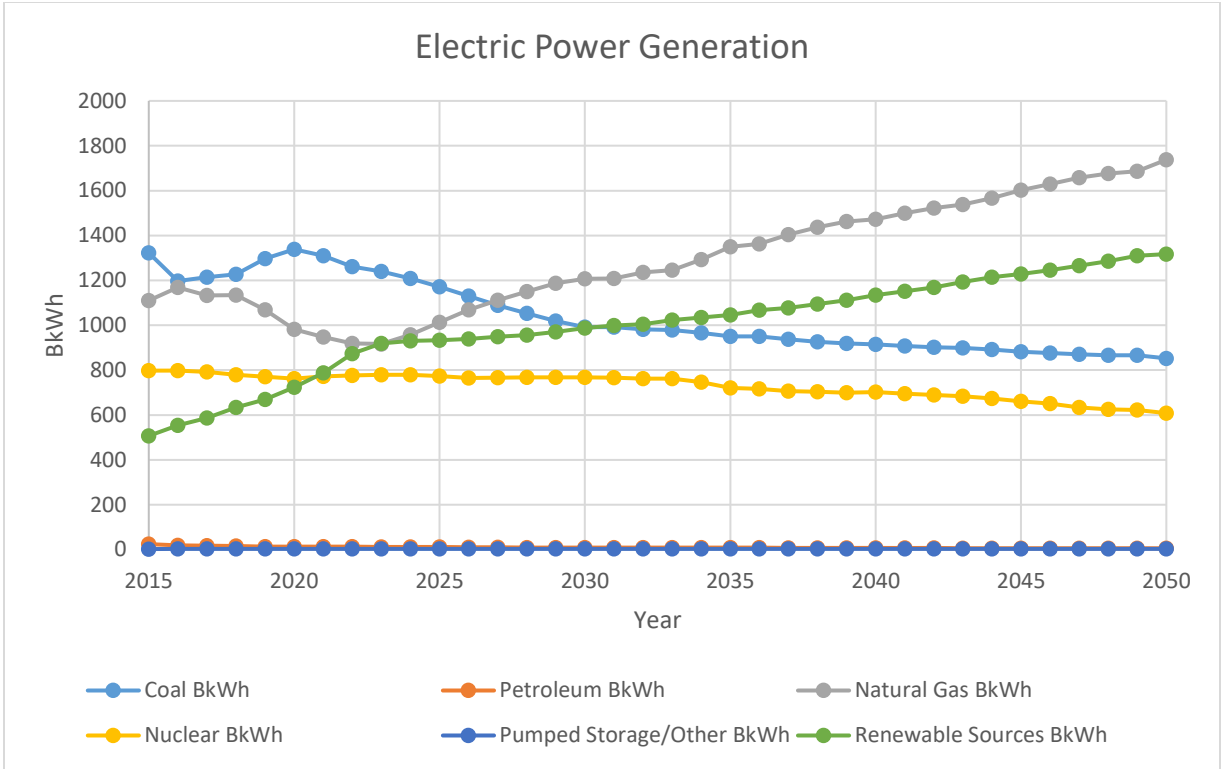


Figure 3. World Power Generation Projects

## 1.2 CHALLENGES POSED BY GENERATION CHANGE TO THE MACROGRID

With the increased penetration of renewable energy comes the need for increased reserve, additional equipment, and revamped protection [1]. Renewables are intermittent by nature. Due to sporadic weather patterns, such as clouds or variable wind, large solar or wind farms can produce maximum power one minute and no power the next. Fossil fuel based generation either cannot ramp up and down fast enough to supply the difference or is too costly to do so; therefore, batteries have become more important as renewable sources are being depended upon more [6]. Battery technology is still developing and not at the point yet where mass installation is seen in many parts of the country. However, it is expected that commercial and industrial energy storage power

capacity capability will grow from 500 MW in 2016 to 9 GW in 2025 [6]. Solar and wind farms are developed in areas where the resources, sun and wind, are most abundant. This could mean wind turbines in the Atlantic Ocean are supplying homes in land locked areas far away. Power electronic based high voltage direct current (HVDC) transmission and flexible alternating current transmission system (FACTS) technologies will need to be implemented to assure consistent power delivery [1]. These systems are expensive, and any issue that causes disturbance in performance could mean the difference between mega-watts (MW) and no power delivery. Because the new generation sources when interconnected are power electronic based, and not SM based, protection techniques conventionally used for the traditional grid are becoming ineffective for specific reasons. Reverse power flow and smaller fault currents, among other issues, are driving a revamping of grid protection techniques [7]. As mentioned earlier, decreasing grid inertia is also a looming issue that must be dealt with.

### **1.3 CHALLENGES POSED RENEWABLE ENERGY TO MICROGRIDS**

Microgrids (MGs) are regulated by IEEE 1547 due to the DG introduced to the system by the MG. In this standard are thresholds for voltage, frequency, and phase values that must be adhered to in order for the MG to be allowed to connect to the macrogrid. Renewable energy, power electronic based generation, is favorable for MG due to environmental reasons but poses challenges when adhering to IEEE 1547. Due to its intermittent nature, controlling the voltage, frequency, and phase of renewable energy and the converter is not simple. This, included in the fact that MG are naturally less rigid grids and feel greater effects from grid disturbances, makes research in the area of renewable generation extremely important.

## **2.0 BACKGROUND**

MG are seen as a way to facilitate DG integration, enhance resiliency, and provide efficient power supply to isolated or remote areas [1][7]. Renewable sources are popular in MGs, especially isolated and remote MGs, due to the readily available supply of sun and wind. Voltage-sourced converter (VSC) based inverters, used to create alternating current (AC) voltage, utilize phase-locked loops (PLL) to synchronize to a desired frequency and phase. Interfacing converters utilizing these PLLs lack the inertial dynamics inherent to SM generation, which can result in grid instability. DG inverters utilizing Virtual synchronous machines (VSM) technology address this instability by mimicking SM inertial dynamics. VSMs are an up and coming control solution to address this instability problem. Replacing a PLL with the swing equation gives VSCs inertia.

### **2.1 DISTRIBUTED GENERATION**

For the purposes of this work, DG units will be divided into two categories, electronically coupled and rotating machines. Electronically coupled DG (ECDG) use a DC to AC VSC, also known as an inverter, to interface between a DC power supply and the grid [7]. Solar-photovoltaic (PV), batteries, type-4 wind-turbine generators (WT), and medium/high speed gas-turbine-generators are examples of power supplies to connect to the grid via VSCs [7]. VSCs often use PLLs to synchronize to the grid, which can make them susceptible to grid instability issues, as they are dependent on a reliable input from the grid.

Rotating machine DG units produce AC voltage by design. Examples include type-1 and type-3 WT, diesel generation units, and low-speed gas-turbine-generators [7]. Rotating machines naturally synchronize their frequency with the grid due to their inherent characteristics, which are described in the swing equation. The frequency stays stable during grid disturbances but the phase angle will increase from the nominal grid phase angle during fault scenarios [8].

## **2.2 MICROGRIDS**

According to the Department of Energy, a MG is a group of interconnected loads and distributed energy resources within clearly defined electrical boundaries that acts as a single controllable entity with respect to the grid [6]. It can connect and disconnect from the grid to enable it to operate in both grid-connected or islanded mode [9]. An example MG can be seen in Figure 4. The point of common coupling (PCC) is the point where the MG can connect or disconnect, island, from the macrogrid depending on system needs. Generation and load is dispersed throughout the MG, meaning power flow has a variable direction. DG units and loads within the MG are equipped with local controllers (LCs) and communicate with the MG supervisory controller and energy management system [7].

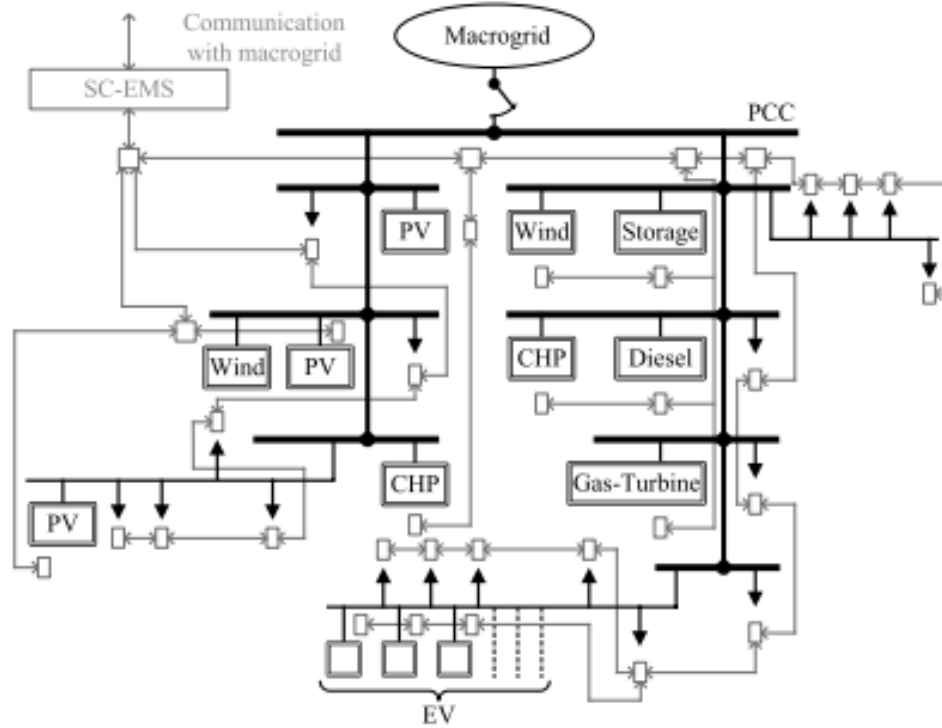


Figure 4. MG example

MG benefits include integration of smart grid technologies, enhanced integration of DG, supply of critical loads, and more [7]. These benefits are very attractive but are not without their challenges. The first being initial cost of the MG [3]. There many technical challenges as well, including reliable operation and control, energy storage, and communications [7].

MG designs also offer the ability to be AC and/or DC. AC designs are the most common and are the focus of this work. DC MG designs offer many benefits but will not be discussed within the scope of this work.

In order to use renewable energy in an AC MG, inverters are needed to convert power from DC to AC, or AC to AC in the case of frequency mismatch. Power electronic inverters are used to make these transformations. Of significant note to this work, these inverters perform the frequency synchronization to the grid and/or load to supply power. This is typically done by utilizing PLLs to synchronize their frequency and phase to the input measurements of the surrounding system.

Due to the direct dependence upon the surrounding system, conventional PLLs lack inertia inherent to the SM. This can pose a frequency instability issue when a MG is operating in islanded mode and does not possess, or at least possesses a low percentage of, rotating sources [5]. The VSM is a solution to this problem, whose research continues to grow in popularity. The VSM is a control method that mimics the inertial dynamics inherent to a SM and is performed by implementing the swing equation into the control of a VSC inverter in order to determine the frequency and phase of DG operation. The VSM can be used in place of the conventional PLL.

### **2.3 VOLTAGE SOURCE CONVERTER**

PWM is a common control method for inverters that utilize phase,  $\Theta$ , and angular frequency,  $\omega$ . PWM utilizes voltage, current, frequency, and phase values extracted from the grid, as seen in Figure 5. These signals are used in the PWM equation to create reference signals, as seen in Figure 6. The reference signals are then compared against triangular wave forms, Figure 7, which results in 1s or 0s, creating the PWM signal, Figure 8. The PWM signal are used to control the gates of the VSC's IGBTs, Figure 5. The IGBTs then switch between on and off states and the output signal is filtered via inductors and a capacitor. Thus, transforming a DC input into an AC output. All variables used in PWM control are in per unit (p.u.).

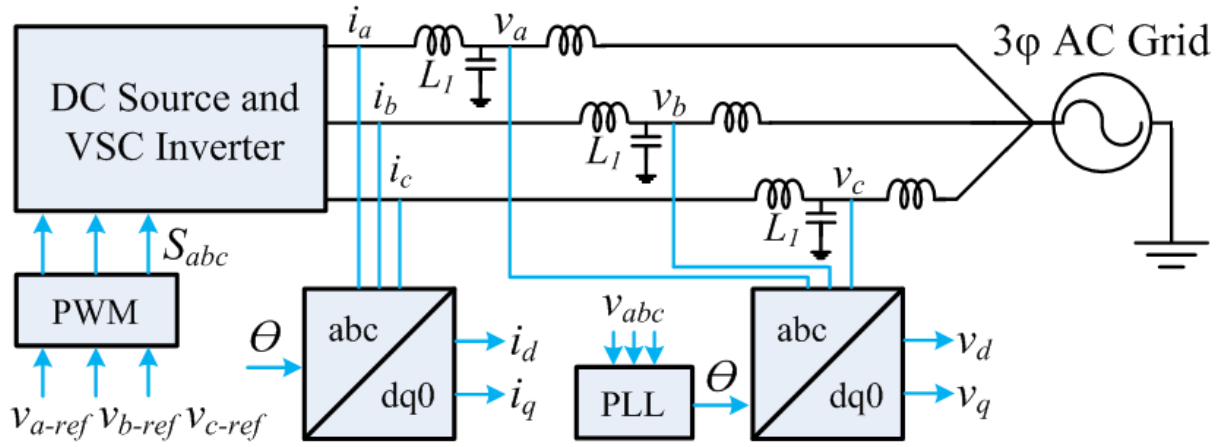


Figure 5. Voltage, current, frequency, and phase values extracted from the grid

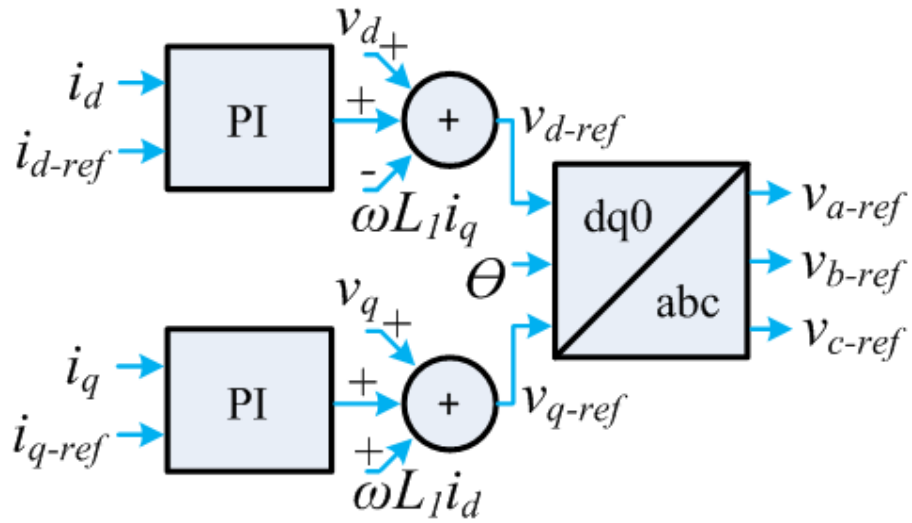


Figure 6. PWM Diagram



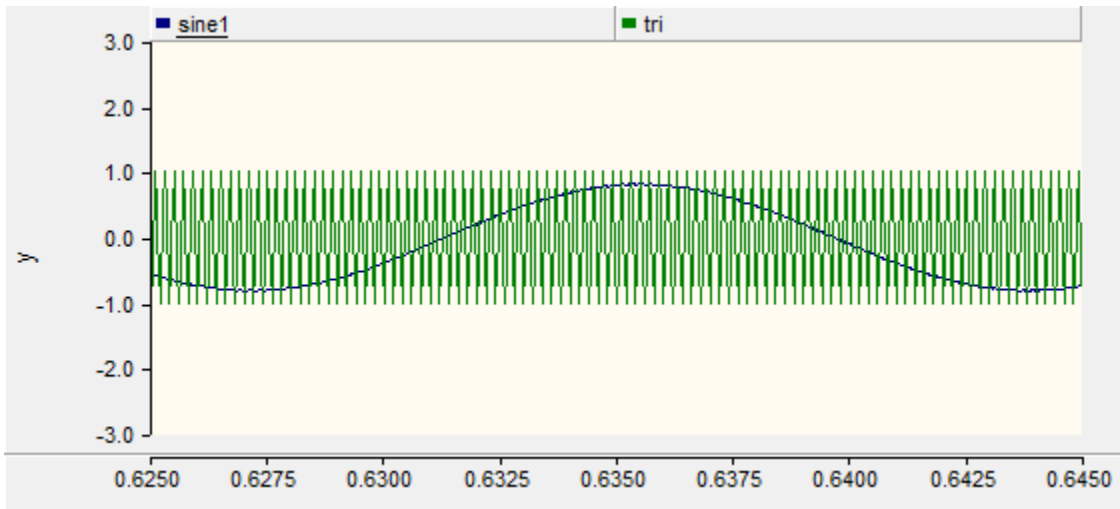


Figure 7. Phase A reference signal Vs. Triangular wave

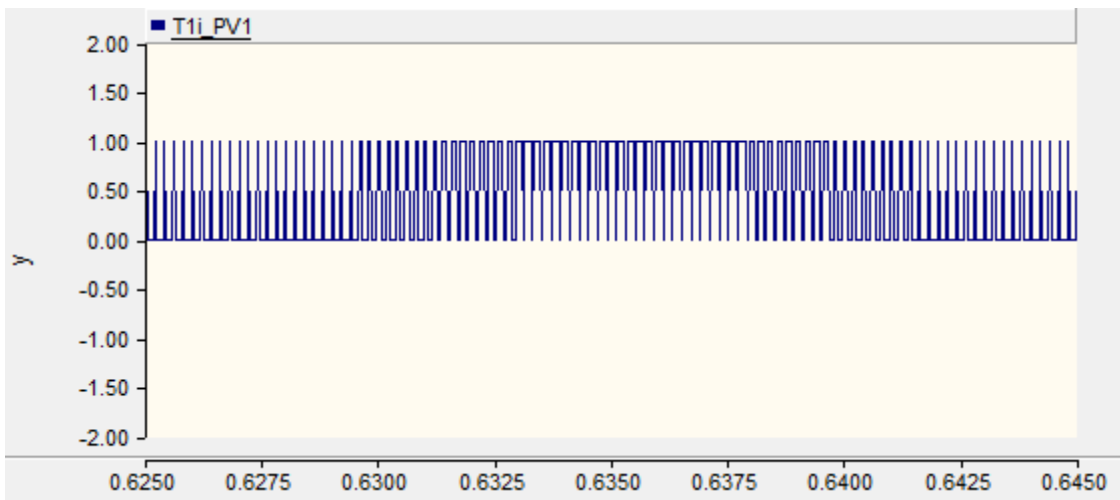


Figure 8. PWM signal that results from phase A reference signal Vs. Triangular wave

## 2.4 PHASE-LOCKED LOOP

A PLL is a nonlinear negative feedback control system that synchronizes its output in frequency, as well as its phase, with its input [10]. PLLs are now widely used for the synchronization of converters and also for monitoring and control purposes in different engineering fields [10].

$$\omega_{pll} = \omega_{grid} + (kp * \tan^{-1}(vq)) + \int ki * \tan^{-1}(vq) \quad (1)$$

The equation that dictates the control of the PLL is given in (1). A diagram representation this (2) can be seen in Figure 9. This PLL is the standard for three-phase applications and is the building block of advanced forms of PLLs [10].

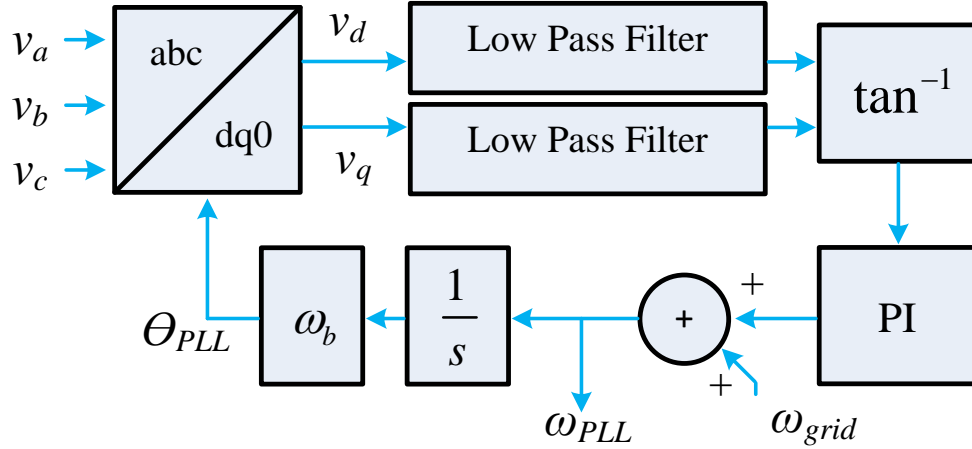


Figure 9. Schematic diagram of the conventional SRF-PLL

PLLs are a great tool to utilize when implementing renewable energy into a strong grid [11]. The PLL is designed to adapt its frequency and phase to that of its input, the surrounding grid. The downfall of the PLL is that it has low inertia and weak dampening [5]. As the ratio of PLL controlled inverters to SM generation increases, the overall inertia of the grid will decrease and be more susceptible to stability issues [5].

## 2.5 VIRTUAL SYNCHRONOUS MACHINE

The SM has long been the king of power generation. The inherent physics of SM dictate the electrical frequency of the voltage, which is locked in fixed proportion to the mechanical rotation speed of the generator, see Appendix A for proof [12]. This means a variation in frequency on a bus directly reflects in the rotational speed of the SM connected to it. The nature of AC power transmission is such that it is only in stable equilibrium if each generation source attached is operating at the same unified frequency [12]. These two facts create two underlying grid control problems: 1) Stable dynamic performance is needed such that any non-SM generation can converge to steady-state in a stable fashion. 2) The frequency must be regulated around 60 Hz. The SM naturally satisfy both of these control issues, which gave great importance to deriving the associated swing equation from its design.

Applying the swing equation to the control of an inverter allows an inverter to mimic the dynamic stability of a SM. These inverters are controlled in such a way to replicate the inertial dynamics inherent to the SGs and are called VSM. Instead of using a PLL in order to synchronize DG to the grid frequency, the swing equation (2) is implemented in the inverter control.

$$\ddot{\theta} = \left(\frac{1}{J}\right) * (T_m - T_e - D_p * \dot{\theta}) \quad (2)$$

This implementation is done in order for the inverter to act as a SM with corresponding damping and virtual inertia, meaning it will not be able to instantaneously change system conditions.

To adapt the equation to inverters, the mechanical and electrical torque are changed to power reference and power output, respectfully. The implemented controls can be seen in Figure 10.

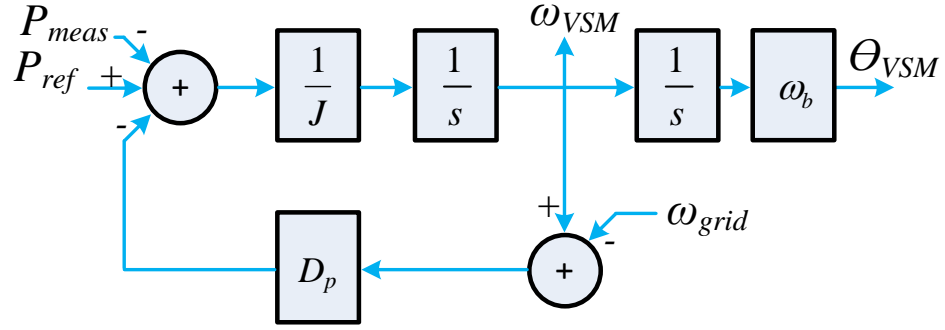


Figure 10. Swing Equation Control for an Inverter

SMs have mechanical inertia and damping through moving parts and friction, where VSMs use inertia and damping constants,  $J$  and  $D_p$ , as modifiable control variables to mitigate or enhance the effects of the system inputs. However, while inertia and damping are fixed in a SM design, the control constants in a VSM can be altered according to the VSM's intended purpose. This flexibility can be very useful benefit in situations but potentially harmful in others. As mentioned before, fault conditions cause SM phase angles to increase due to the nature of the swing equation. This holds true for VSM implementation as well.

### 3.0 MICROGRIDS

As noted earlier, MGs offer many benefits in industrial, commercial, and residential power systems but they are complex systems. Figure 11 shows how intricate MGs can be. In order to have an efficient system, variety of generation sources, energy storage, and utility connection is needed. Still, the enhanced reliability, peak shaving, and efficient supply in remote areas are a few benefits that make this complexity a small sacrifice [1]. Technical challenges, such as the stability of the frequency, control algorithms, protection techniques, and generation sources, create new challenges and opportunities for engineers.

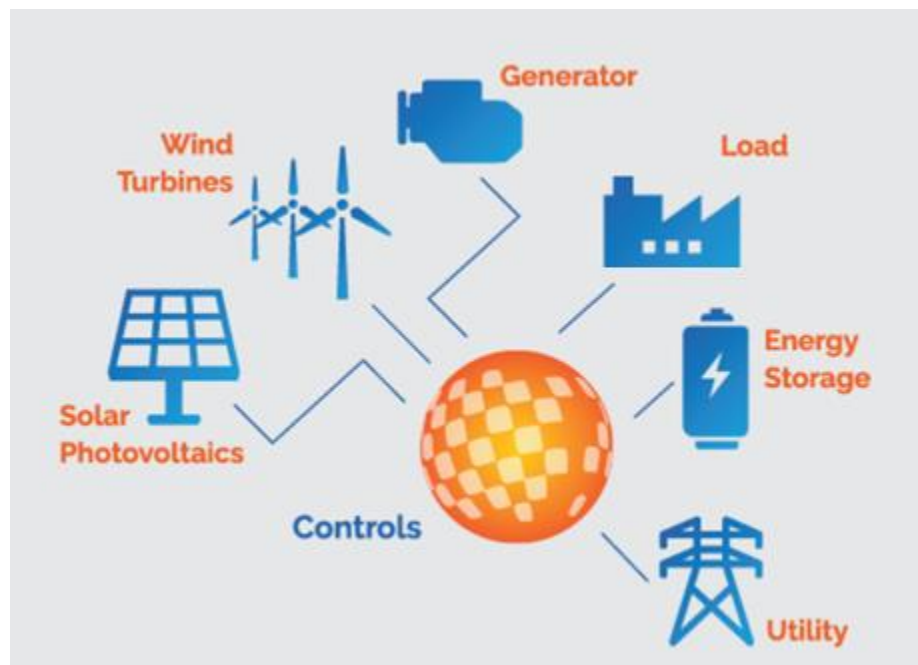


Figure 11. Components of a MG

## **3.1 TYPES**

### **3.1.1 Urban**

Urban MG are located in a populated or a concentrated industrial area. The feeders are densely loaded, giving them a low degree of voltage imbalance [7]. During the grid-connected mode of an urban MG, the voltage and frequency are dictated by the macrogrid. Therefore, DG units within the MG can be synchronized with relative ease, which is of importance for protection [7].

### **3.1.2 Rural**

Rural MG are located in a sparsely populated area, meaning the load is scattered. In a rural MG, voltage imbalance and fluctuation can be significant. Thus, DER units have impact on voltage, and if permitted, can be controlled to assist in the feeder voltage regulation [7].

### **3.1.3 Off-grid**

Off-grid MG, by definition, always operates in islanded mode. Because there is no possibility for macrogrid connection, an off-grid MG does not comply with the strict definition of “microgrid”. They do not connect to the macrogrid because are geographically located in a remote area or surrounded by difficult terrain for transmission line connection. Integration of large-size DG units with off-grid MGs is occurring at faster and higher pace than urban and rural MGs, due to the immense need for voltage stability from each DG unit [7].

## **3.2 DESIGN**

### **3.2.1 Control**

MGs have inherent characteristics, such as a high degree of imbalance and the diversity of DG units, which pose challenges to devise a viable control for all operating scenarios [7]. Also, MG are required to transition between grid connected and islanded mode, further complicating MG control. To satisfy MG needs, four main levels of control are used, grid-interactive, supervisory, local area, and device-level [13]. These levels can be implemented via hierarchical control then customized using centralized or decentralized control [7].

#### **3.2.1.1 Four Main Hierarchical Control Levels**

MG control can be broken down into four main hierarchical levels, from the top level moving down: Grid-interactive control (GIC), supervisory control (SC), local area control (LAC), and device-level control (DLC) [13]. GIC's functions include area electric power system (AEPS) control, electricity markets consideration, and more. SC functions are less broad as it controls generation and load dispatch, optimization, spinning reserve, and other facets of the MG. LAC's function is to balance generation and load, while also considering disconnection and resynchronization needs. Lastly is DLC, which is the lowest level of control. Here, among other functions, voltage and frequency control is performed, as well as islanding and fault protection, and energy storage control. These four levels of control work together from top to bottom to ensure the MG operates smoothly, works efficiently, and can safely and effectively interact with the main electric grid.

### **3.2.1.2 Centralized Vs. Decentralized Control**

Centralized and decentralized control are two very distinctly opposite approaches when it comes to the architecture of a MG's control. A fully centralized control relies on data gathered in a central controller that performs all calculations and determines the actions for all units at the single point [14]. This requires extensive communication to receive and send out control signals. Decentralized control relies on each unit being controlled by its own local controller, making it unaware of system-wide variables [14].

Both strategies have advantages and disadvantages. Interconnected power systems usually cover extensive area, making a fully centralized approach infeasible due to the vast communication it would require [14]. However, a system comprised of entirely decentralized control is also infeasible as the coupling need between various units requires a certain degree of communication [14].

The solution is to make a compromise, integrating both strategies at varying degrees. This can be done using a hierarchical control scheme consisting of three levels: primary, secondary, and tertiary [14]. The higher level operations use centralized control for grid-level specific parameters while the lower level operations use decentralized control for dispatch, coordination, and converter level control decisions [14].

### **3.2.2 Protection**

Carefully designed MGs can be major assets to the improvement of grid resilience. However, the offered resilience is seriously undermined if MGs are not properly protected in the event of faults within their own boundaries [7]. Three main characteristics of MG make conventional protection



techniques used by the macrogrid ineffective. First, the fault current levels of MG are much different in islanded mode in contrast to grid connected mode. Second, the diversified generation profile available and common to MG, as well as the complex operating scenarios, require more intricate and custom protection than the macrogrid. Third, VSC interfaced DG exhibit unconventional fault behavior [7]. These challenges offer a great number of research opportunities and will need to be investigated more fully before MG become widespread in the grid.

### **3.2.3 Generation**

SMs currently dominate the main grid, but it is typically an invalid assumption that MG generation profiles mimic the main grid [7]. SM are an important part of the MG generation profile due to the need for reliable operation and the intermittency that results from renewable energy sources. IEEE Standard 1547 sets guidelines for DG to follow. These standards are applied to DG simulation behavior later in this work. For inquiries not addressed in this work, IEEE 1547 and its appendixes can be examined to learn more about DG behavior in MG.

## **4.0 MICROGRID PROTECTION PROJECT**

MG protection is an area that deserves more attention than it receives. MGs are often lauded for their resiliency capabilities. Their resiliency is compromised if they cannot successfully protect their own assets. Also, it is found that any SM will incur phase angle increases during grid events, making it more difficult for MG to move freely between grid connected and islanded mode [8][15]. There are no commercially available MG protection relays, causing MG owners to use traditional relay techniques, such as directional overcurrent, distance, and differential [7]. These techniques have been staples of the protection of the macrogrid but their performance has not been thoroughly analyzed in MGs as of yet.

### **4.1 MICROGRID ISLANDING EXPERIMENTATION**

As stated previously, MG can improve system resilience, but this is greatly undermined if they are not properly protected. In the case of a fault, it is incredibly important that the MG can island itself safely so that it can continue to supply the loads within its boundary and assist with black start, if need be. Due to popularity and intermittency of renewable energy sources, thorough islanding strategies are needed to stabilize the islanded management of generation and load.

In order to examine the phenomena of smooth MG islanding, simulations were completed using Real Time Digital Simulation (RTDS) Hardware-in-the-loop (HIL). Multiple islanding strategies were considered for testing. Slave Master Operation (SMO) uses a single inverter as the voltage and frequency reference. In SMO mode a single inverter can be used as a voltage reference

when the main power supply is lost and the other power sources can operate in PQ mode [16]. Load shedding is another widely studied MG islanding strategy. In a scenario in which the islanded MG does not have enough generation to power the entire load, any non-critical loads are disconnected when possible, also known as load shedding [17]. Another recently developed strategy is power sharing within a network of MG. In this strategy, grid connected MG export power to other MG in order to balance the load management [18].

This project performed and presented here in this work used a MG islanding strategy most resembling SMO. The MG has PV generation that partially powers the load in grid-connected mode. Once islanded additional generation will be brought online to supply the necessary power to satisfy the load. RTDS was used to implement relay coordination, sending trip signals in order to achieve the purpose of an extremely accurate islanding time measurement. It goes without saying that speed is of the utmost importance for effective islanding operation.

#### **4.1.1 IEC 61850 – GOOSE Protocol**

To boost electric utility automation, new devices are constantly being integrated into the grid. Generally speaking, the devices utilized in protection coordination often come from a variety of vendors and thus most protocols do not match each other, making interoperability not possible or very complex. This challenge led to the birth of IEC 61850, also known as GOOSE. GOOSE is an acronym for generic object-oriented substation event. GOOSE provides a solution for interoperability between devices from different vendors. This is accomplished by defining a common set of rules and by defining logical nodes into Substation Automation System (SAS) functions [19]. It uses Ethernet and TCP/IP for communication. Use of Ethernet communication allows the replacement of conventional copper wiring, improving the speed of communication.

Apart from standardizing the electrical utility, the 61850 protocol also supports ‘self-description’ i.e., ability of a device to display its data to a client browsing the device contents. The standard describes standards for client-server and peer-to-peer communications, substation design and configuration, testing, and project implementation [19]. This protection experimentation performed for this work utilized GOOSE messaging for its practical application and speed.

#### **4.1.2 Real Time Digital Simulation - Hardware-in-the-Loop Technology**

HIL has become a very popular method for testing electric grid components. Because the electric grid cannot be physically replicated due to its size, or experimented upon for obvious practical reasons, a simulation program that could incorporate real components into a simulated grid environment became necessary. RTDS is a HIL technology that can react in real time to the equipment it is connected to. RTDS was used in this project because of the need to test the speed of a MG islanding implementation, specifically testing the protective relays to recognize a fault, island a MG, and bring additional generation online.

#### **4.1.3 Procedure**

The MG islanding scheme was inspired by Dominion Energy’s relay logic and communication protocols for tripping DG offline. Within substations that are connected to DG sites, panels are equipped with a SEL-451 and a SEL-735. The SEL-735 is used primarily to monitor total demand distortion (TDD) and the total harmonic distortion (THD). In the event that one of these changes by more than a set percent, it will send a trip signal to the SEL-451 via mirrored bit. The SEL-451 then sends a signal to the SEL-651R at the DG site via fiber optic cables to disconnect the DG.

This project used similar protocol for MG islanding. When disconnected, the MG will not cease to generate but instead it will work to balance generation and load. The SEL-651R will send the trip signal to a SEL-3530, in addition to disconnecting the MG. The SEL-3530 will then send a signal to a SEL-651R to bring more generation online. GOOSE messaging will be used as the primary form of communication to decrease latency.

A model was developed using the RSCAD software. A one-line of the model can be seen in Figure 12. A circuit breaker (CB) is placed between the grid and the PCC. PV, a SM, and load are all connected to the bus. The PV generation is set to supply half of the load, meaning the grid partially powers the load. To test the islanding procedure, multiple relays are attached to the RTDS. The SEL-451, SEL-651R, and SEL-3530 are utilized in this work. A diagram showing the communication between the RTDS and the relays can be seen in Figure 13. A double amplifier is needed to step up RTDS output signals to real values.

Once the equipment is set up, a line-line-ground (LLG) fault is applied to the grid in RSCAD, creating an undervoltage. The SEL-451 monitoring the current will send a trip signal to a SEL-651R when the fault occurs. The SEL-651R then sends the signal to the RTDS, to island the MG. The SEL-651 also sends a signal to the SEL-3530, which sends a signal to another SEL-651R. The SEL-651R then sends a signal to the RTDS to connect the natural gas generator. The natural gas supplies the remaining 200 kW in order to balance load demand and generation. The experimental HIL set up can be seen in Figure 13.

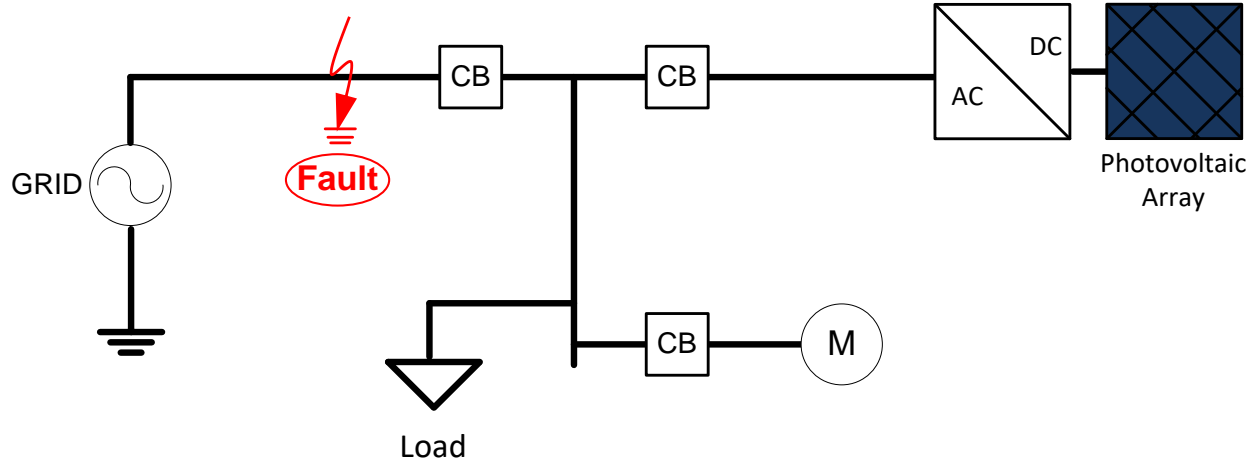


Figure 12. One-line of grid connected MG

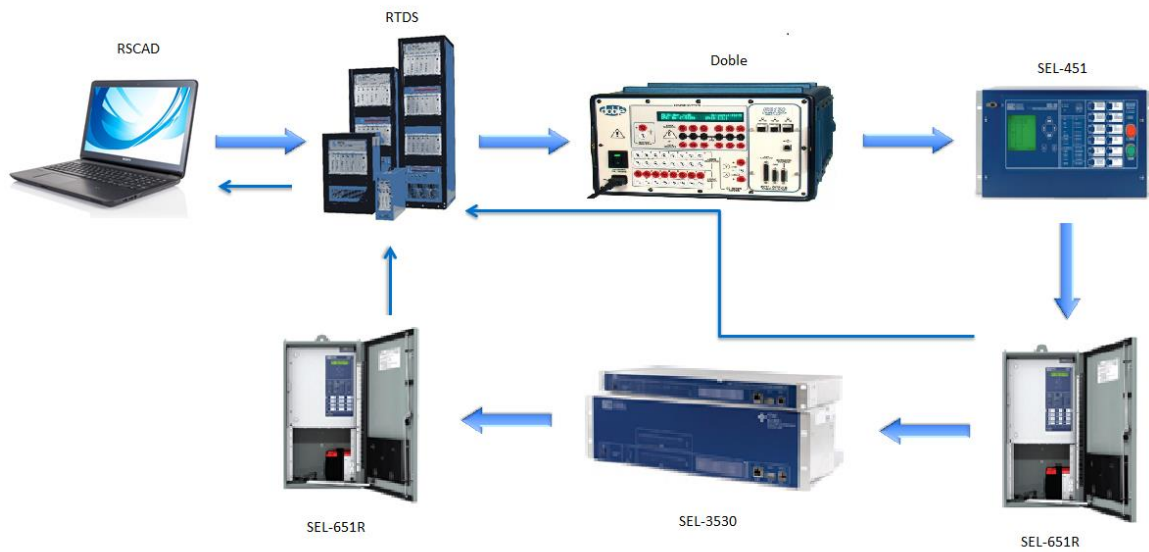


Figure 13. RTDS HIL set up

#### 4.1.4 Results

Here, HIL simulation results is presented to demonstrate the effectiveness of the islanding procedure. A fault was triggered. The effects of this fault can be observed at 0.19992 s, as shown

in Figure 14a. The MG is islanded, via BRKX, at 0.22536 s, as seen in Figure 14b. The delay of 25.92 ms can be attributed to the time the SEL relay takes to recognize the overcurrent and send a signal back to the RTDS. Figure 14c shows that the natural gas generator is brought online at 0.23712 s, 37.2 ms after the fault occurs. The time delay is caused by the relay fault detection, as specified above, and the time needed for the relays to communicate via GOOSE messaging. It takes 12 ms for the fault signal to be sent from the islanding SEL-651R to the MG generation relay (SEL-651R). There is a latency duration of 6 ms for each relay to relay communication. Figure 15 shows the equivalent voltage of the MG before and after the fault. The voltage recovers to 1 p.u. at 0.26184 s, which is 61.92 ms or four cycles after the fault occurs. Figure 16 shows the frequency before and after the fault. The frequency recovers to nominal conditions, 60 Hz, at 0.27336 s, which is 73.44 ms or four cycles after the fault occurs.

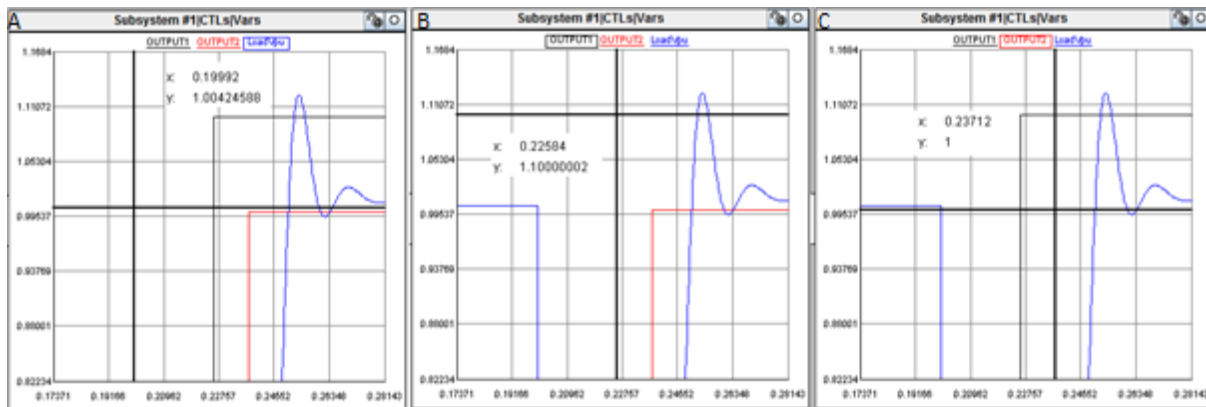


Figure 14. a) Measured time of fault occurrence b) Measured time of MG islanding  
c) Measured time of natural gas generator start up

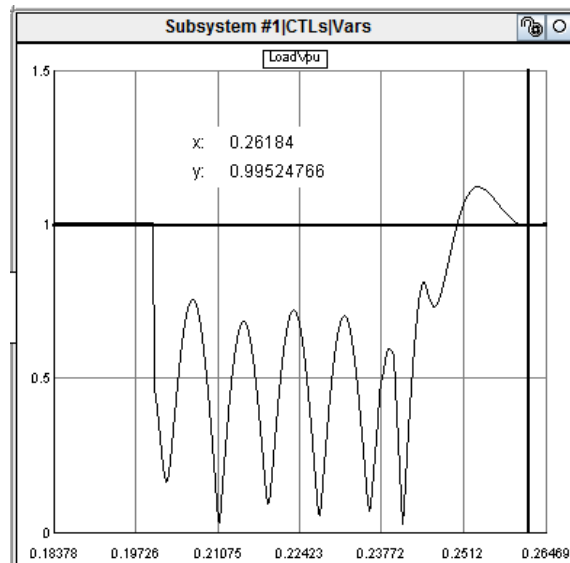


Figure 15. Voltage p.u. islanding results

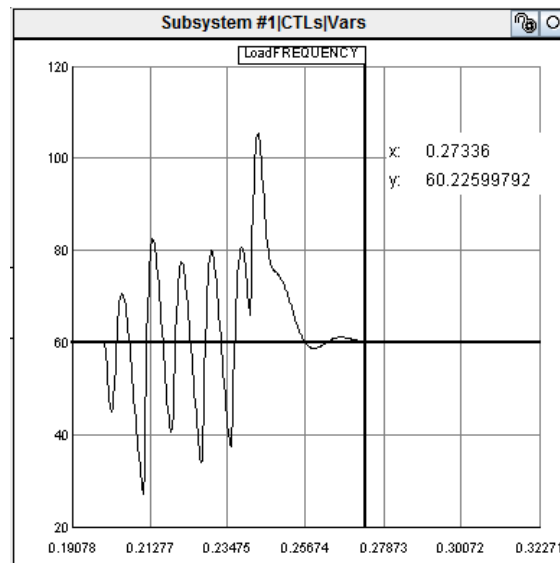


Figure 16. Frequency islanding results

#### 4.1.5 Findings

Dominion Energy's DG tripping scheme was successfully applied to a MG islanding scenario.

Almost half the four cycles needed to correct voltage and frequency came from the generator's



ability to stabilize voltage. Tuning the PI controller of the generator could produce even faster stabilization. The SEL relays and GOOSE messaging accounted for the other two cycles. The small delay of 37.2 ms, is adequate for MG islanding, proving the procedure's ability to recognize fault conditions, island a MG, and bring generation online.

#### **4.1.6 Impact**

The faster a MG can be separated from a fault, the better for the health of the MG. This includes any fuses, relays, loads, and generation sources in the MG. In particular, the SM in the MG. As stated earlier in this work, fault conditions lead to phase angle increases in SM. Fast islanding, such as the times demonstrated in this work, will minimize fault effects on phase angle [8].

## 5.0 VIRTUAL SYNCHRONOUS MACHINE MODELING

The VSM modeling in this paper was done with the guide of [20] and [21] . The swing equation replaces the conventional PLL and can be used in conjunction with any pulse width modulation (PWM) controller. This work uses a current controller in order to ensure the MG load is fully supplied.

### 5.1 PHASE-LOCKED LOOPS

The PLL dates back to 1930s when it was first designed and used for the synchronous reception of radio signals [10]. Since then, it has found widespread applications in different areas, such as the estimation of fundamental parameters, such as phase, frequency, and amplitude, of power signals [10], Figure 5. Conventional PLLs use the 3-phase voltage signals at the inverter terminals as the inputs of the system [10]. A  $dq0$  transformation is then applied to the input to determine the phase difference between the voltage signal and the internal oscillator rotating frame. The difference between the two signals is then put into a PI controller, which produces  $\omega_{PLL}$ .  $\omega_{PLL}$  is then integrated to generate  $\theta_{PLL}$  [10].

PWM uses the outputs of PLLs,  $\theta$  and  $\omega$ , in the controls and parks transformations, as shown in Figure 5. This is because synchronizing to the grid is not inherent to inverters as it is SM. The phase of the grid found via PLL is used in the  $dq0$  to  $abc$  transformation that creates the PWM reference signals.

## 5.2 SWING EQUATION

The swing equation, (2), has been successfully used by power engineers to solve a vast array of problems [22]. Notably, this work can be used to bring stability to non-SM. This work will analyze how the swing equation can be applied to VSCs in order to accommodate the mass penetration of renewables without losing grid inertia and stability. By implementing the swing equation to replace a conventional PLL, a degree of rigidity is added to the operation of the VSC, now called a VSM. This is possible as the objective of a conventional PLL in VSC control is to generate the phase and frequency of the grid, for synchronization purposes. The swing equation naturally does this as it is the driving force behind keeping thousands of SM all over the grid synchronized.

### 5.2.1 Equation Variables

There are three variables in the swing equation that determine the output,  $\ddot{\theta}$ :  $T_m$ ,  $T_e$ , and  $\dot{\theta}$ .  $T_m$  and  $T_e$  represent mechanical and electric torque, respectfully. Rotating machines have torque but power electronic converters do not. Therefore equation (2) will be altered so that torque is replaced with the power reference and power output measured. Power equals the product of torque and speed, or torque and electrical frequency. Frequency usually is successfully regulated to an exceptionally tight band, within 0.5% of 60 Hz. Therefore, power can then be approximated as proportional to torque. Because the controls of VSC occur in per unit, power and torque can be approximated as interchangeable [12]. Frequency analysis in a later section will show that frequency deviation is very limited for VSMs so the assumption that power equals torque will hold.  $\dot{\theta}$ , or angular frequency, on the other hand is simply the integral of the output,  $\ddot{\theta}$ . This acts as a feedback loop to

correct any deviation from the grid's angular frequency. For the purposes of the VSM,  $\dot{\theta}$  is actually  $\dot{\theta}_{VSM} - \dot{\theta}_{grid}$ .

$$\ddot{\theta} = \left(\frac{1}{J}\right) * (P_{ref} - P_{meas} - D_p * (\dot{\theta}_{VSM} - \dot{\theta}_{grid})) \quad (3)$$

Therefore, the equation (3) is used to dictate the phase and frequency of the VSM. A diagram equivalent for (3) can be seen in Figure 17.

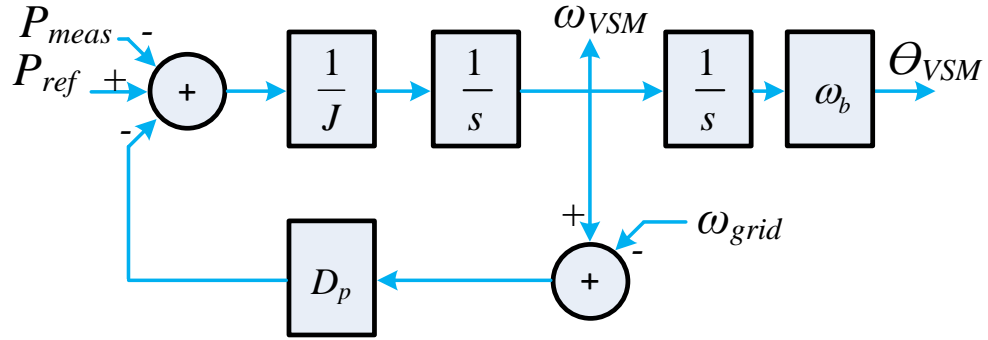


Figure 17. Swing equation altered for VSM control

### 5.2.2 Examine Constants in the Equation

There are two constants in the swing equation that determine the output,  $\ddot{\theta}$ :  $J$  and  $D_p$ .  $J$  is the inertia constant and  $D_p$  is the damping constant [20][21]. In a SM, inertia is related to the size of the machine because larger machines are more difficult to affect.  $D_p$  is the damper winding, which opposes oscillations incurred by the machine and creates a torque to oppose any speed change [23]. These values are usually intrinsic to a SM but in a control system, the user has the flexibility to change their values. This is advantageous as increasing or decreasing either constant gives the user options to design the behavior of the VSM. The larger  $J$  is, the less of an impact  $P_{ref}$ ,  $P_{out}$ ,

or  $D_p^*(\dot{\theta}_{VSM} - \dot{\theta}_{grid})$  will have on the system output. This is to say that the larger the system inertia, the less inputs can affect the system.  $D_p$  only affects the difference between  $\dot{\theta}_{VSM}$  and  $\dot{\theta}_{grid}$ . This is to say that any difference between the two is magnified so that it is corrected as fast as possible. This comes from the inherent property of SM to stay synchronized to the grid.

### 5.2.3 Constants Have a Large Impact on System Performance

Three scenarios will be examined to show how altering the values  $J$  and  $D_p$  can affect the operation of a VSM. The following procedure will be used for each scenario. First the VSM will attach to the grid at 0.4s, where it will supply 0.5 p.u. to the load. Then at 0.7s the main grid will disconnect and the VSM will supply 1.0 p.u. to the load. Finally, a 1.0s a fault will be applied to the load for 0.1s. The system frequency, in p.u., will be analyzed to determine the effects of altering the constants  $J$  and  $D_p$ .

First a “control” example will be examined where  $J=2$  and  $D_p=25$ . For the second example,  $J$  will be reduced to 1.1 and  $D_p$  will be kept at 25.  $J$  is chosen to be 1.1 instead of 1 because an inertia value of 1 would mean there is no inertia. For the last example,  $J$  will be returned to a value of 2 and  $D_p$  will be increased to 50.

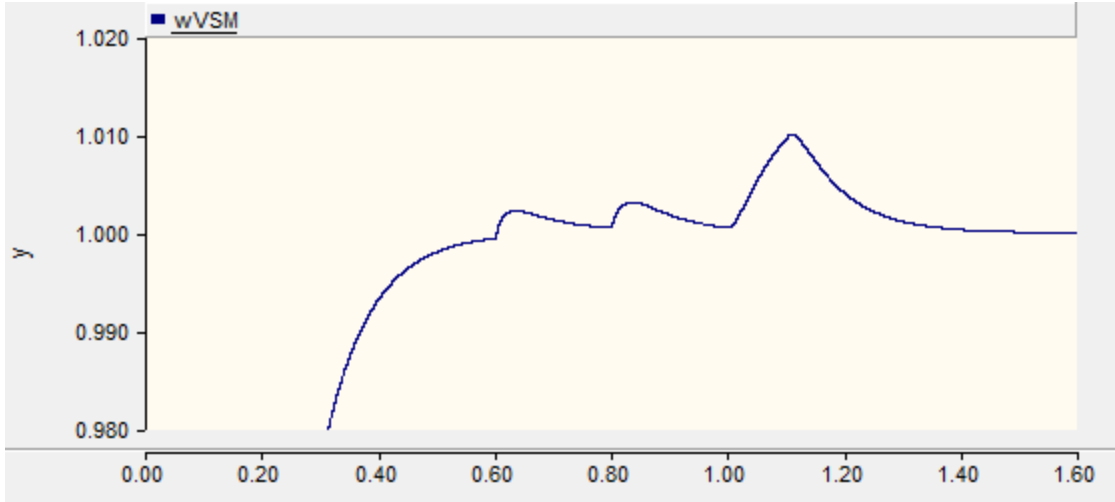


Figure 18. Frequency results for  $J=2$  and  $D_p=25$

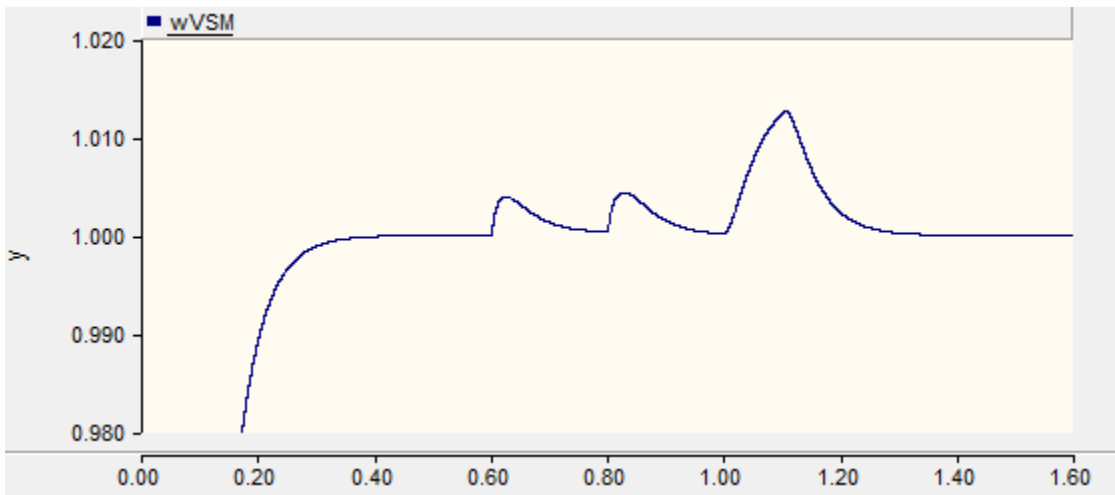


Figure 19. Frequency results for  $J=1.1$  and  $D_p=25$

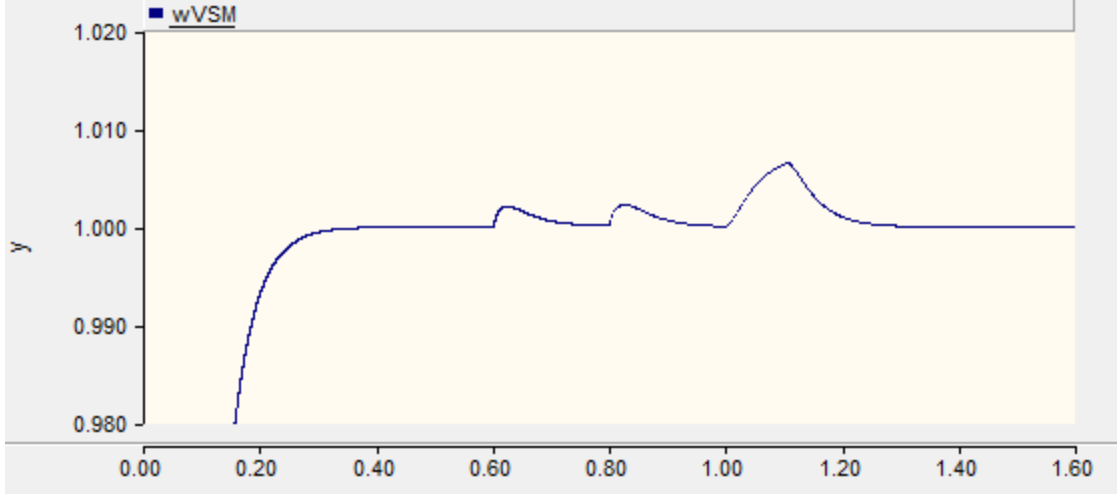


Figure 20. Frequency results for  $J=2$  and  $D_p=50$

Figures 18, 19, and 20 show that altering the constants of the swing equation has a major effect on the frequency of a VSM. When  $J$  is decreased from 2 to 1.1 the effects of power reference change and fault application is mitigated. When  $D_p$  is increased from 25 to 50, the effects of grid events are also mitigated but to a larger degree.

This can be explained by observing that both  $P_{ref}-P_{out}$  and  $\dot{\theta}_{VSM}-\dot{\theta}_{grid}$  are in per unit. But  $\dot{\theta}_{VSM}-\dot{\theta}_{grid}$  is amplified by the dampening constant,  $D_p$ , giving it a much larger impact on the frequency of the VSM.  $P_{ref}-P_{out}$  moves the frequency away from the nominal 60 Hz but  $\dot{\theta}_{VSM}-\dot{\theta}_{grid}$  corrects the frequency back to 60 Hz. Therefore decreasing  $J$  will allow for  $\dot{\theta}_{VSM}-\dot{\theta}_{grid}$  to have a larger effect but also allows  $P_{ref}-P_{out}$  to have a larger effect as well. However, increasing  $D_p$  amplifies the effect of  $\dot{\theta}_{VSM}-\dot{\theta}_{grid}$  and does not affect the effect of  $P_{ref}-P_{out}$ . This shows that increasing both variables,  $J$  and  $D_p$ , has a positive effect on minimizing the difference between VSM frequency and the grid frequency but  $D_p$  has a larger impact.

## **6.0 VOLTAGE AND FREQUENCY ANALYSIS**

When a new control method is being explored it is only natural to compare it to the long-standing method that has been relied on extensively in the past. Therefore, the VSM must be compared to the conventional PLL to determine if this unique control solution is truly better than the current solution. If the VSM cannot show that it at least matches the conventional PLL's performance then it has no hope to become relevant in power generation. However, if the VSM can show it is superior to the conventional PLL in voltage, frequency, or phase stability, then there are possibilities for it be implemented readily. This section will test the conventional PLL and VSM by bringing a VSC online, synchronizing it with the grid, increasing power output, islanding the VSC, and applying a fault. This will occur in three instances, VSM alone, conventional PLL alone, and when they are combined in parallel. The voltage and frequency results will then be compared against IEEE 1547 to determine if the VSM offers improvement over the conventional PLL.

### **6.1 TESTING PROCEDURE**

Table 1 outlines the values used in the following simulation. This included values for the VSC's filter,  $D_p$  and  $J$  constant values for the VSM, and the resistive value of the load. The locations of the filter impedances can be seen in Figure 5.



Table 1. Parameter values for VSC filter, VSM, and grid load

Parameter	Value
$L_1$	11.3 mH
$C_1$	26.5 uF
$L_2$	229 uH
$D_p$	2
$J$	50 kg*m <sup>2</sup>
$R_{Load}$	4.8 Ohm

The simulation will start and allow time for the system to synchronize to the grid. At 0.35 s the VSC will attach itself to the grid. Then, at 0.4 s, the power reference will raise to 1.0 p.u., or 0.5 p.u. each in the case of the parallel example. At 0.6 s the VSC and load will island from the main grid. A L-G fault is applied to the load at 1.0 s for a duration of 0.1 s. A breakdown of the simulation events can be seen in Table 2.

Table 2. Grid events and corresponding times

Event	Time (s)
Connect VSC to main grid	0.35
Increase power reference from 0.0 p.u. to 1.0 p.u.	0.4
Island MG	0.6
Apply fault	1.0
Clear fault	1.1

## 6.2 TESTING CRITERIA

IEEE 1547.4 states that, when in island mode, DG power quality must be acceptable to all parties [1547DG][15]. IEEE 1547 abnormal voltage and frequency standards for DG<30kW will be used

to deem if the power quality is acceptable or not and ultimately determine if the inertia given to the inverter via the VSM has an impact on fault recovery [24].

Table 3. Abnormal voltages

Voltage range (% of base voltage)	Clearing time (s)
$50 \leq V \leq 88$	2.00
$110 < V < 120$	1.00

Table 4. Abnormal frequencies

Frequency range (Hz)	Clearing time (s)
$> 60.5$	0.16
$< 59.3$	0.16

Tables 3 and 4 state the abnormal voltage and frequency levels for which DG must trip off line when grid connected [24]. These values will be used to judge the VSM's ability to recover from a grid disturbance. These values were defined for the safety of the inverter and it should trip off line if it cannot recover from a grid disturbance to a point within these ranges of  $0.88 \text{ p.u.} < V \text{ p.u.} < 1.1 \text{ p.u.}$  and  $59.3 \text{ Hz} < \text{Frequency} < 60.5 \text{ Hz}$  [24]. If the inverter's power quality is not within these ranges, it will be deemed unacceptable.

## 6.3 RESULTS

### 6.3.1 Conventional Phase-Locked Loop

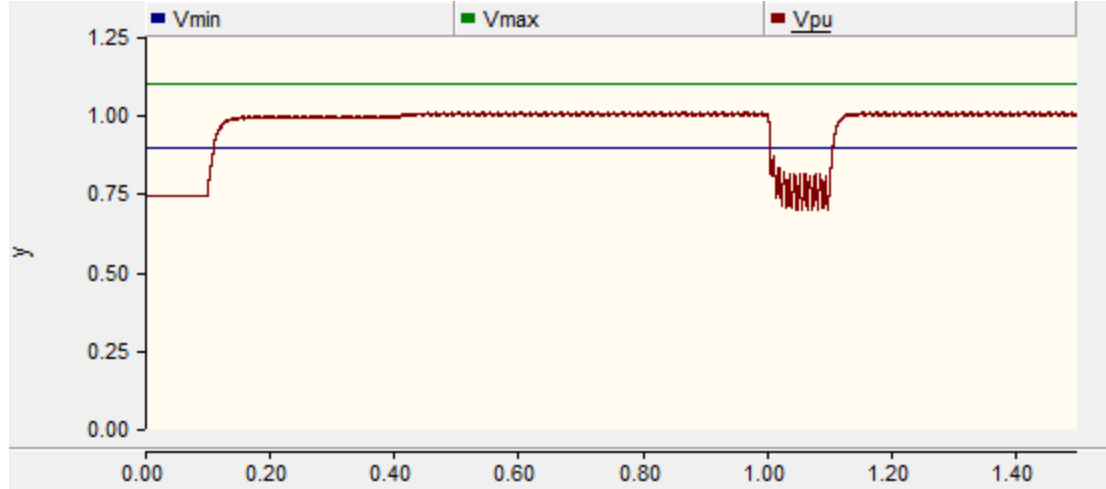


Figure 21. Voltage response of a VSC controlled by a conventional PLL

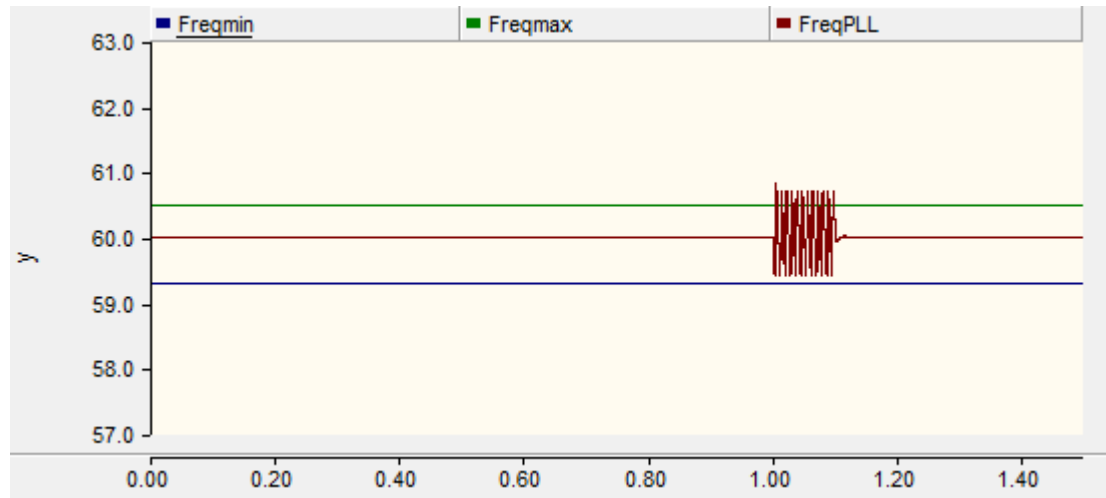


Figure 22. Frequency response of a VSC controlled by a conventional PLL

Figures 21 and 22 show the voltage and frequency response of a PLL controlled VSC during the events described in Table 2.

### 6.3.2 Virtual Synchronous Machine

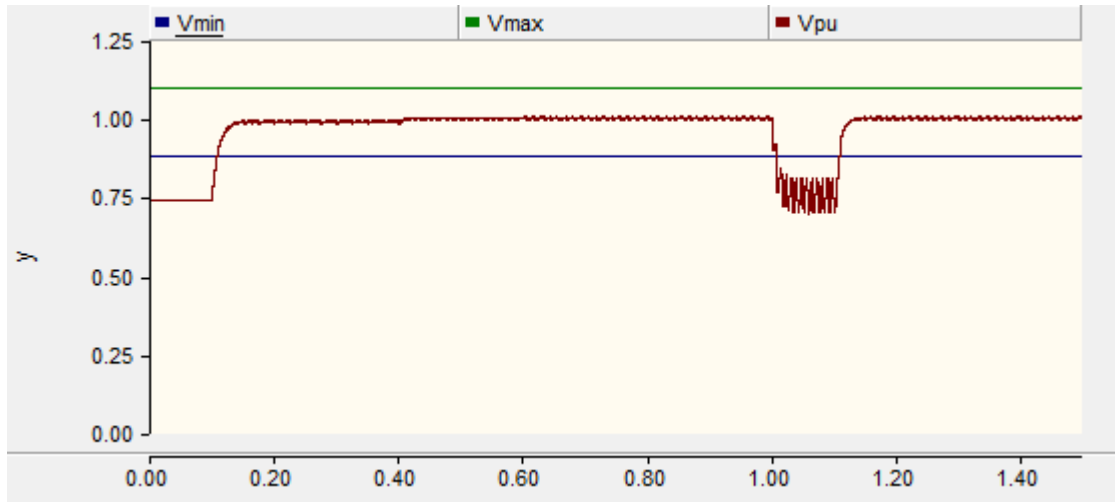


Figure 23. Voltage response of a VSC controlled by a conventional PLL

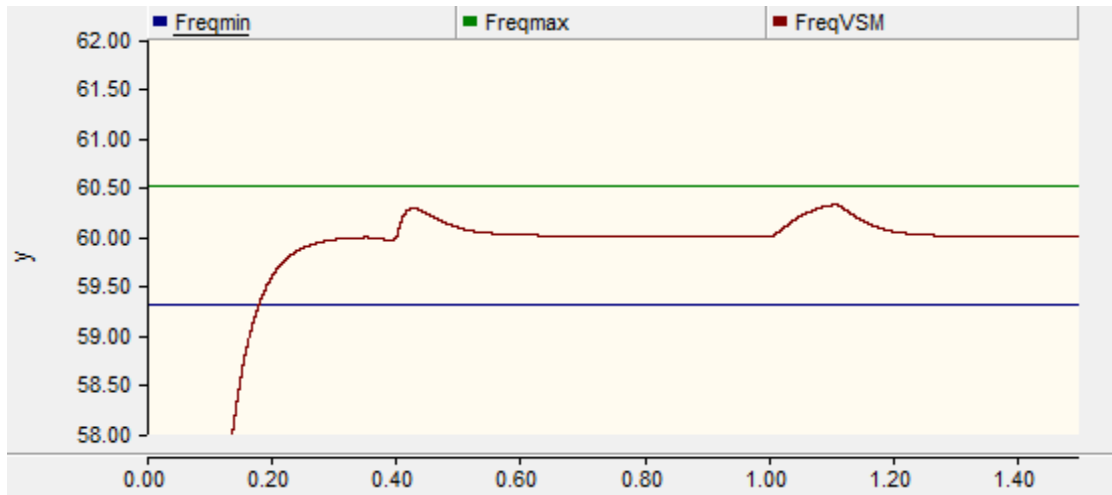


Figure 24. Frequency response of a VSC controlled by a conventional PLL

Figures 23 and 24 show the voltage and frequency response of a VSM during the events described in Table 2.

### 6.3.3 Parallel Combination of Conventional Phase-Locked Loop and Virtual Synchronous Machine

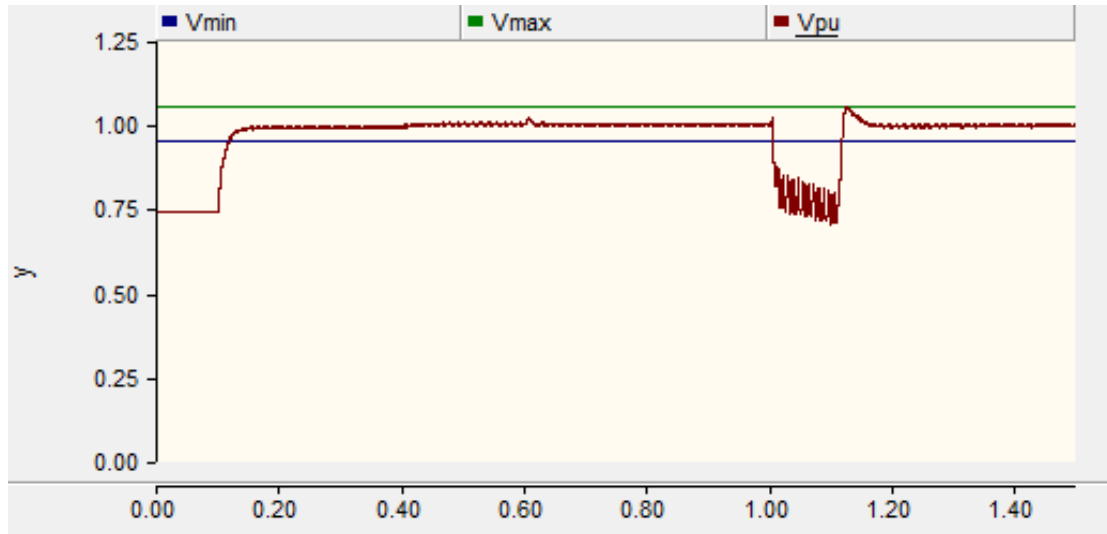


Figure 25. Voltage response of parallel VSC controlled by a convention PLL and a VSM

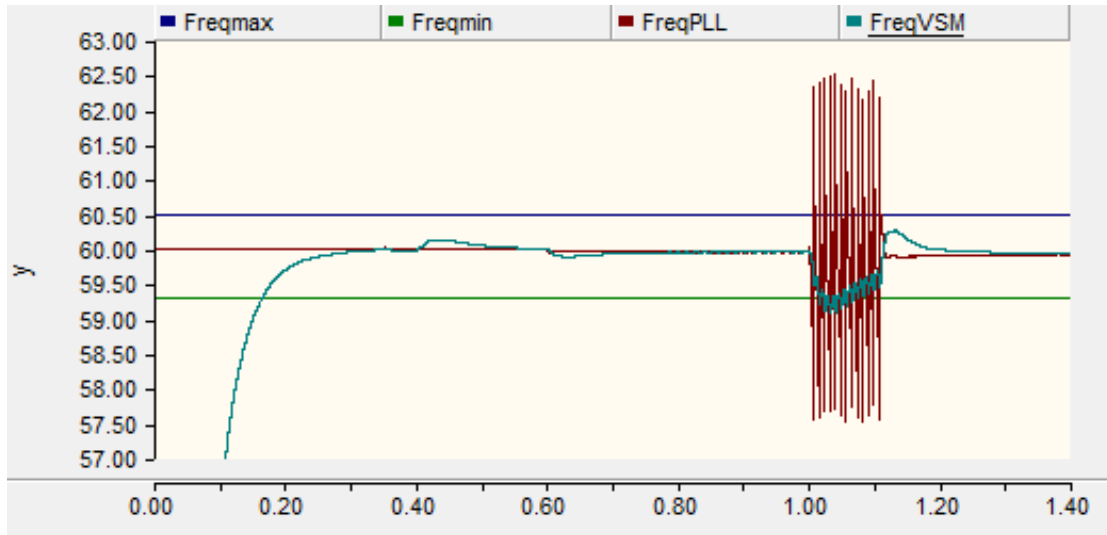


Figure 26. Frequency response of parallel VSC controlled by convention PLL and VSM

Figures 25 and 26 show the voltage and frequency response of PLL and VSM controlled VSC during the events described in Table 2.

## **6.4 ANALYSIS**

Figures 21, 23, and 25 show that the system voltages stabilize within the limits defined by IEEE 1547 in all three scenarios. This is expected as the controls are set to fully supply the load's power based on a specified current. Because real power is a product of current and voltage, and both power and current are controlled, the voltage will be too. Figures 22, 24, and 26 show that the inverter frequency in all three scenarios stabilizes after the fault is cleared. The frequency of the inverter controlled by the conventional PLL leaves the IEEE 1547 limits during the fault in both scenarios it is used in. However, the conventional PLL's frequency is much more volatile when in parallel with the VSM. The frequency of the VSM controlled inverter does not leave the limits in either scenario.

## **6.5 PERFORMANCE DISCUSSION**

Figures 24 and 26 show that the VSM's frequency never leaves the predefined frequency limits. The inertia of the VSM keeps the frequency from deviating outside of the predefined range. This is the main area where the VSM performance differs from the conventional PLL's. Figures 22 and 26 show that the conventional PLL's frequency will oscillate around 60 Hz during the fault. This affect is amplified when in parallel with the VSM. That is because in the stand-alone scenario the input signal for the conventional PLL is its own output but in the parallel scenario the input is both its output and the output of the VSM, which are not synchronized during the fault.

The VSM's dampening and inertia keep it from instantaneously changing values, unlike the conventional PLL, which attempts to synchronize to its input, regardless of input quality.

## **7.0 PROPOSED PHASE CORRECTION**

A key factor to power quality is phase angle. It is often forgotten about due to the importance put on voltage and frequency stability. This work has already shown that voltage is dependent on the system's PWM method and the VSM improves frequency stability. This section will focus on the VSM's phase because, unlike voltage and frequency, VSM phase does not have any self-correction method. PWM is given reference signals and the dynamic PI controller works to correct the output to these levels, correcting the voltage. The swing equations main objective is to correct the error between the grid's frequency and the VSM's frequency.

The swing equation shows that the phase angle is the integral of the system's frequency. If the system was stable and the only change to the frequency was raising and lowering the power reference, then the system's phase angle would not deviate too far from its set point. Unfortunately, the power grid is not a perfect utopia. Grid events such as faults, frequency drops and more must be anticipated. When any of these events occur the frequency, and consequently the phase angle, will change. If a drastic enough event occurs, the phase may be too far away from the main grid's nominal phase, causing power quality issues and overall system instability.

### **7.1 TEST PROCEDURE**

IEEE 1547 sets limits for the frequency, voltage, and phase angle of a system that must be abide by in order for a system to synchronize to the main grid. These limits can be seen in Table 5 [24].

Table 5. Synchronization frequency, voltage, and phase limits defined by IEEE-1547

Aggregate rating of DG units (kVA)	Frequency difference ( $\Delta f$ , Hz)	Voltage difference ( $\Delta V$ , %)	Phase angle difference( $\Delta\theta$ , degrees)
0-500	0.3	10	20
>500-1500	0.2	5	15
>1500-10,000	0.1	3	10

This section will test the VSM's ability to stay within these ranges while in island mode. Though these limits do not directly say MG sources must abide by the, they are a great starting point to make sure MG DG generation is stable. Three scenarios will be tested: A conventional PLL in parallel with a VSM, two VSMs in parallel, and two VSMs in parallel with a phase correction method implemented. To test this, the following simulation procedure will be used. First, a start-up period from 0.0s to 0.3s where the phase angles are held constant. Second, the power references of the DG sources are increased. Third, the MG islanded from the main grid. Fourth a fault is applied and removed. The phase angle will then be examined to determine the effects.

## 7.2 CONVENTIONAL PLL AND VIRTUAL SYNCHRONOUS MACHINE IN PARALLEL

A test scenario will be run using the conventional PLL and VSM to show that when in island mode the conventional PLL will synchronize to the VSM, as the VSM is the strongest generation source in the MG. A representation of the simulation set up can be seen in Figure 27.

The simulation begins in a start-up period from 0.0s to 0.3s where the phase angle of the VSM is held at the grid phase until the VSM is properly synchronized. At 0.3s the power references



of each VSC are increased from is raised from 0.0 p.u. to 0.5 p.u.. Then, at 0.5s, the MG is islanded. A line-to-line fault is applied at 0.7s across phase A and phase C. The fault is cleared at 0.85s. The phase angle difference will be examined once the procedure is completed.

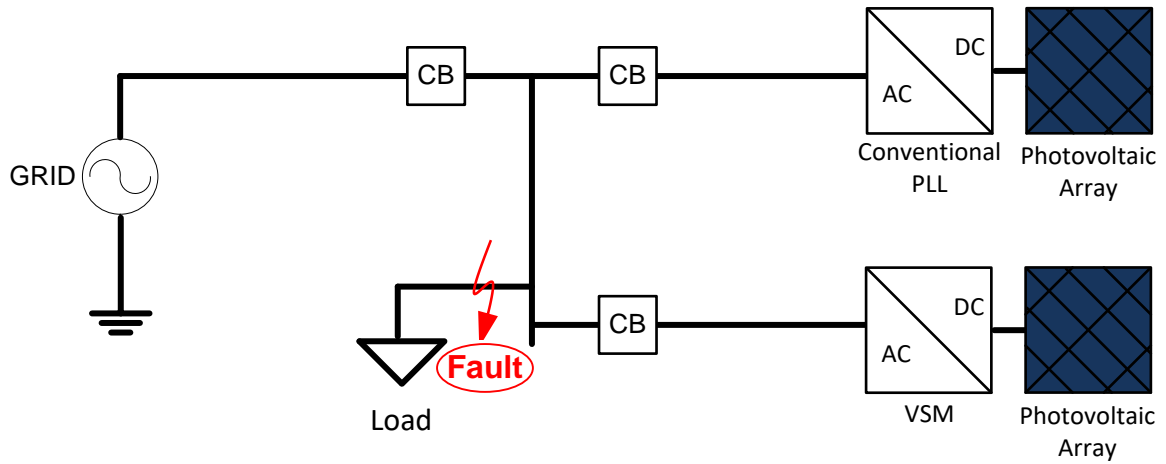


Figure 27. Conventional PLL and VSM in parallel MG set up

Table 6. Events and corresponding times

Event	Time (s)
Connect VSCs to main grid	0.3
Increase each power reference from 0.0 p.u. to 0.5 p.u.	0.3
Island MG	0.6
Apply fault	0.7
Clear fault	0.85

### 7.2.1 Results

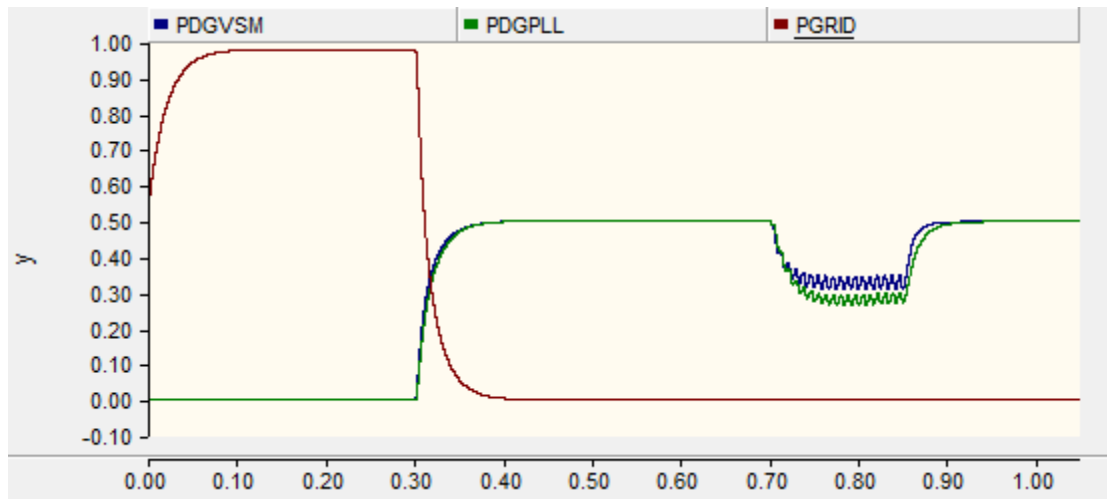


Figure 28. Per unit power output of conventional PLL and VSM

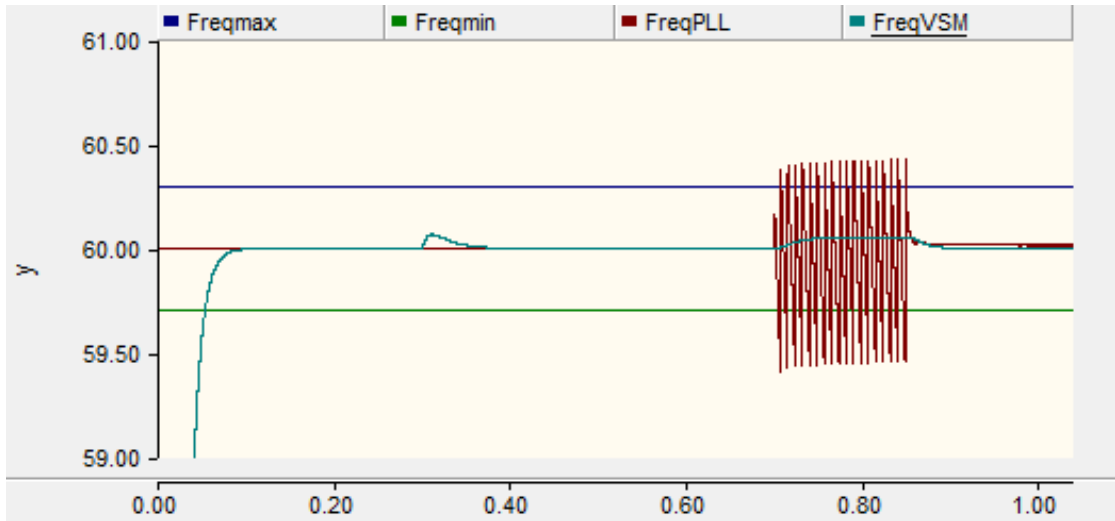


Figure 29. Frequency results of the conventional PLL and VSM

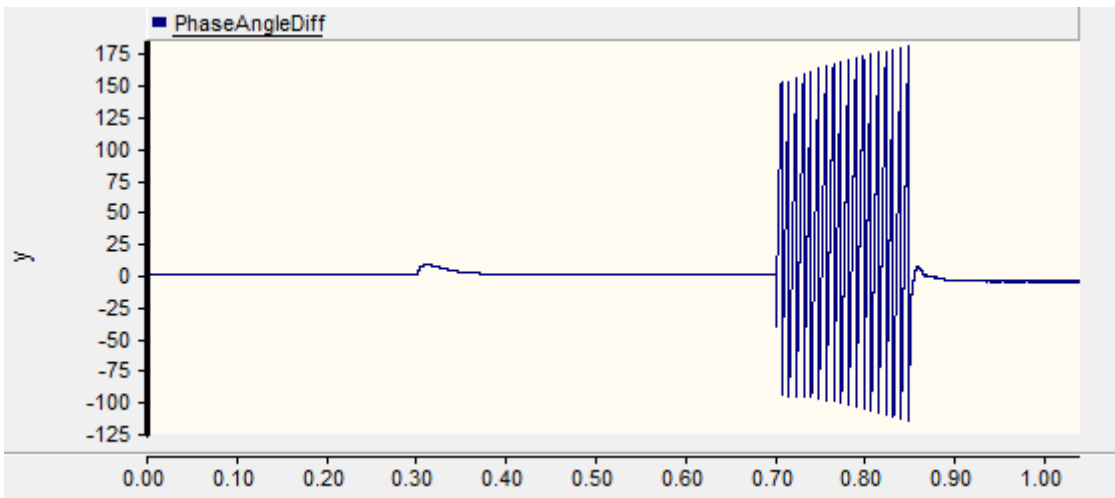


Figure 30. Phase angle difference in degrees

Figures 28, 29, and 30 show the power output, frequency, and phase difference of PLL and VSM controlled VSCs in island mode during the events described in Table 6.

### 7.2.2 Analysis

The swing equation shows that power out vs. power reference alters the frequency of the VSM. Therefore frequency changes seen in Figure 29 are directly proportional to the differences between power reference and output power seen in Figure 28.

As expected, the conventional PLL synchronized to the strongest source it was connected to. While in grid connected mode, this was the main grid. When in island mode this was the VSM. This is shown by the frequency results in Figure 29. During the VSM's frequency gain during power out ramp up, the conventional PLL does not deviate from 60 Hz because the main grid does not deviate from 60 Hz. However, once the main grid is disconnected, the conventional PLL synchronizes to the VSM. This is seen in Figures 29 and 30, as during and after the fault the conventional PLL attempts to synchronize to the VSM's frequency and phase angle. During the duration of the fault the conventional PLL's frequency oscillations slightly increase, just as the VSM's frequency does. Then, once the fault is cleared, the conventional PLL synchronizes to the frequency of the VSM.

Also, the conventional PLL's phase angle synchronized to the VSM's phase angle. This is because the conventional PLL uses a  $dq0$  transformation for synchronization. When the  $q$  component is 0 then the synchronization is complete. This also means that the source is in phase with its reference.

### 7.3 PARALLEL VIRTUAL SYNCHRONOUS MACHINES

A test scenario will be run with two VSMs and no phase correction technique to show the difference in VSM phase that can arise after grid events. To do this, the VSMs are designed with different operational goals. VSM1 is designed so that the grid's parameters will have a large impact on its own parameters. VSM2 is designed to prioritize maintaining nominal grid frequency in all scenarios. The corresponding design parameters chosen for these operational goals are shown in Table 3.

They will also be given different power references in order to differentiate the work needed to raise power out to power reference. A representation of the simulation set up can be seen in Figure 31.

The simulation begins in a start-up period from 0.0s to 0.3s where the phase angles of the VSMs are held at the grid phase until the VSMs are properly synchronized. At 0.3s the power references of VSM1 and VSM2 are increased from 0.0 p.u. to 0.9 p.u. and 0.1 p.u., respectfully. Then, at 0.5s, the MG is islanded. A line-to-line fault is applied at 0.7s across phase A and phase C. The fault is cleared at 0.85s. The phase angle difference will be examined once the procedure is completed.

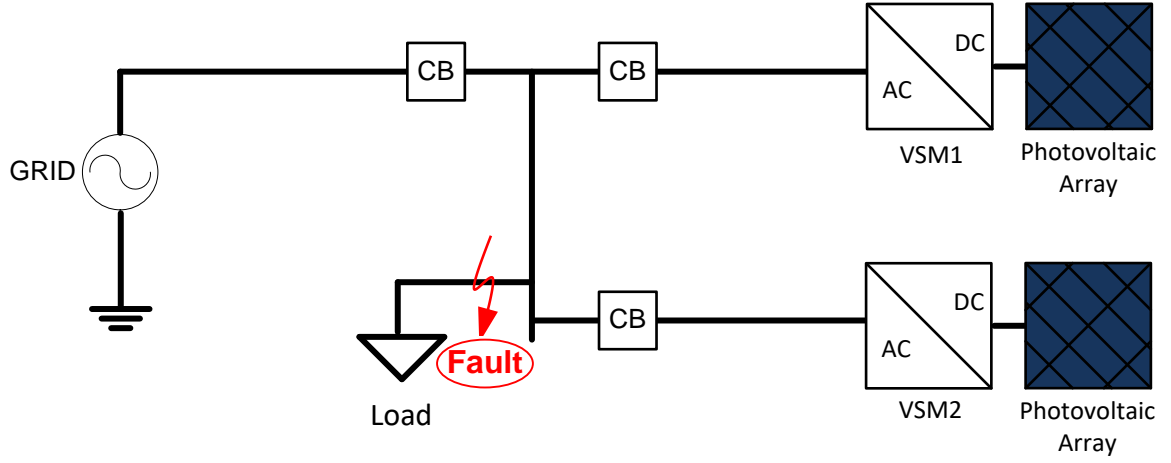


Figure 31. Parallel VSM MG set up

Table 7.  $D_p$  and  $J$  values for VSM1 and VSM2

Parameters	VSM1	VSM2
$D_p$	60	400
$J$	1.1	3

Table 8. Events and corresponding times

Event	Time (s)
Connect VSMs to main grid	0.3
Increase power reference 1 from 0.0 p.u. to 0.9 p.u.	0.3
Increase power reference 2 from 0.0 p.u. to 0.1 p.u.	0.3
Island MG	0.6
Apply fault	0.7
Clear fault	0.85

### 7.3.1 Results

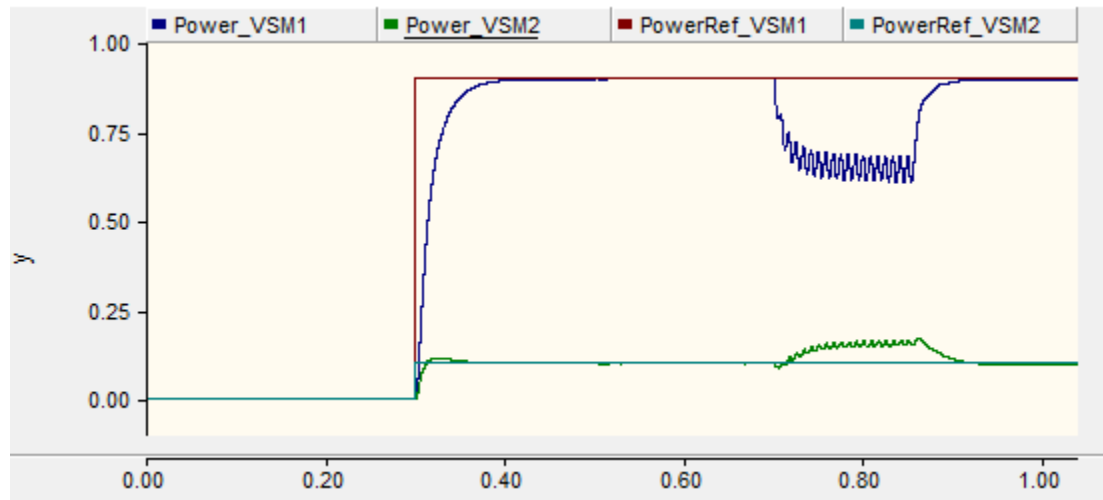


Figure 32. Per unit power output parallel VSM

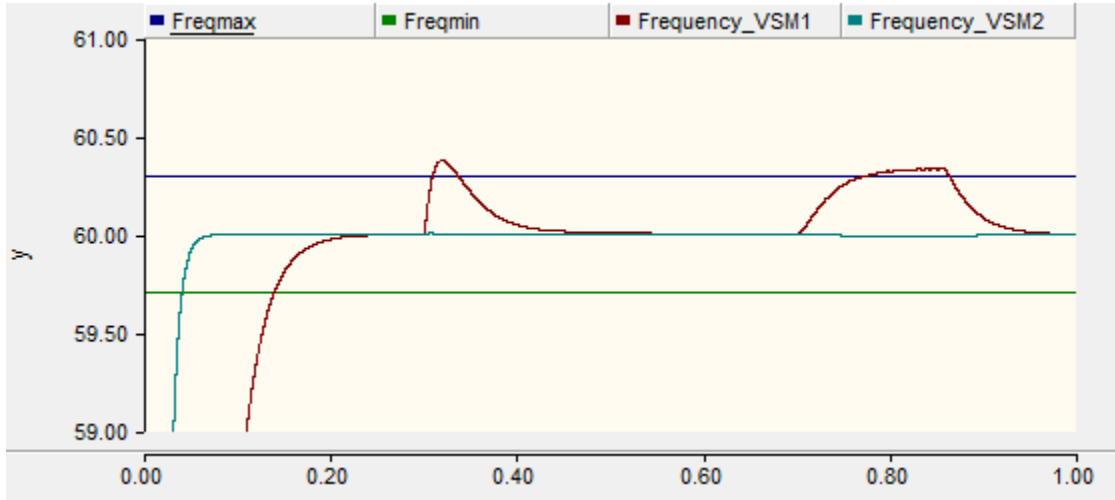


Figure 33. Frequency results of parallel VSMs

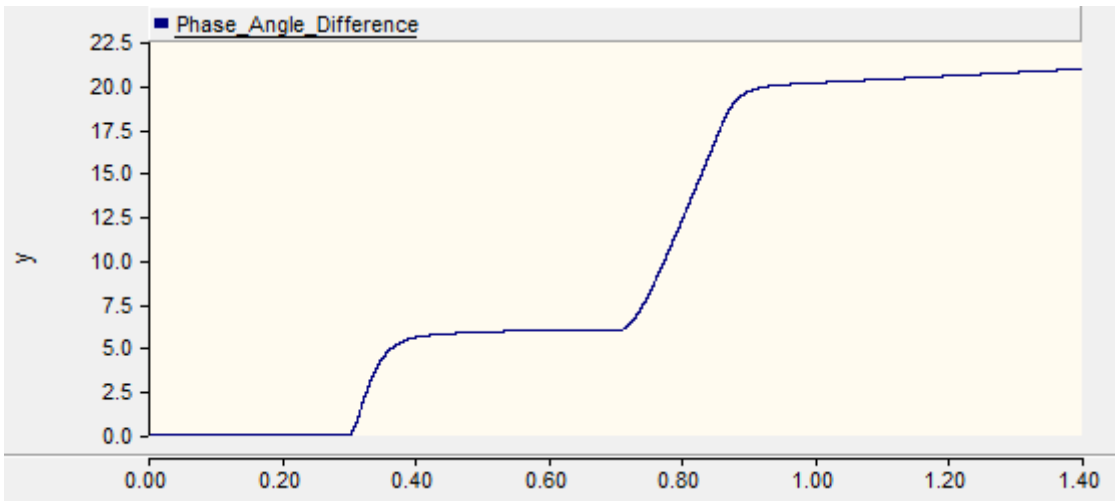


Figure 34. Phase angle difference in degrees

Figures 32, 33, and 34 show the power output, frequency, and phase difference of parallel VSM controlled VSCs in island mode during the events described in Table 6.



### 7.3.2 Analysis

The swing equation shows that power out vs. power reference alters the frequency of the VSM. Therefore the power out, seen in Figure 32, is directly proportional to the frequency change seen in Figure 33.

As expected, VSM1's frequency was greatly influenced by the grid events. The smaller  $D_p$  and  $J$  values not only impacted the phase of VSM1 during these events, they made it impossible for VSM1 to completely synchronize back to the reference, 60 Hz. Once the error between the grid and VSM frequency was small enough, the control loop was no longer strong enough to correct it, due to the lower constants. This can be observed in Figure 34.

Therefore, not only did the grid events have a large impact on the phase difference, the fault recovery conditions created an ongoing phase difference increase due to the slight frequency difference between the systems.

## 7.4 DIFFERENCES

These two examples show exactly why VSMs are needed on the grid but also why more research and preparation is needed before they can be integrated on a mass scale. The two simulations show perfectly that conventional PLLs lack inertia, while the implementation of the swing equation gives VSCs inertia. The conventional PLL finds the strongest generation source and synchronizes to it. If there is too much conventional PLL controlled generation on the grid then there would be fewer strong stable sources to synchronize to. As the frequency of these sources diminish the effect of any error or fault on strong generation is amplified and mimicked by more and more power

electronic generation. This increases the severity of grid mishaps. However, the conventional PLL does resynchronize to strong sources, limiting the phase angle difference and therefore power quality issues.

The reference of a VSM has much less effect on the VSM. VSMs are affected by the system input and behave according to their system design, and only synchronize frequency to another source after substantial input time. The previous simulation showed that the frequency of the VSM is affected much less than the frequency of the conventional PLL. However, the VSM currently lacks a way to synchronize itself back to nominal phase angle, possibly creating power quality issues.

## **7.5 CORRECTION**

Phase displacement is a serious issue for DG because if the phase displacement is large enough then the system will become unstable. An example of this and a phase correction algorithm are demonstrated in this section.

### **7.5.1 Grid Instability**

The parallel VSM example from the previous section was allowed to run for 5 seconds to show the instability that will occur. This is illustrated in Figures 35 and 36. The phase angle increase and voltage decrease are inversely proportional. The phase angle continues to grow in a linear fashion until around 3 seconds where it becomes exponential, showing instability. The same can be said for the voltage as it slowly decreases in a linear fashion then exponentially accelerates. The

voltage leaves the IEEE limits at 4.4 seconds, which correlates to a phase difference of 64 degrees. The voltage continues to fall as the phase difference continues to grow, both at exponential rates.

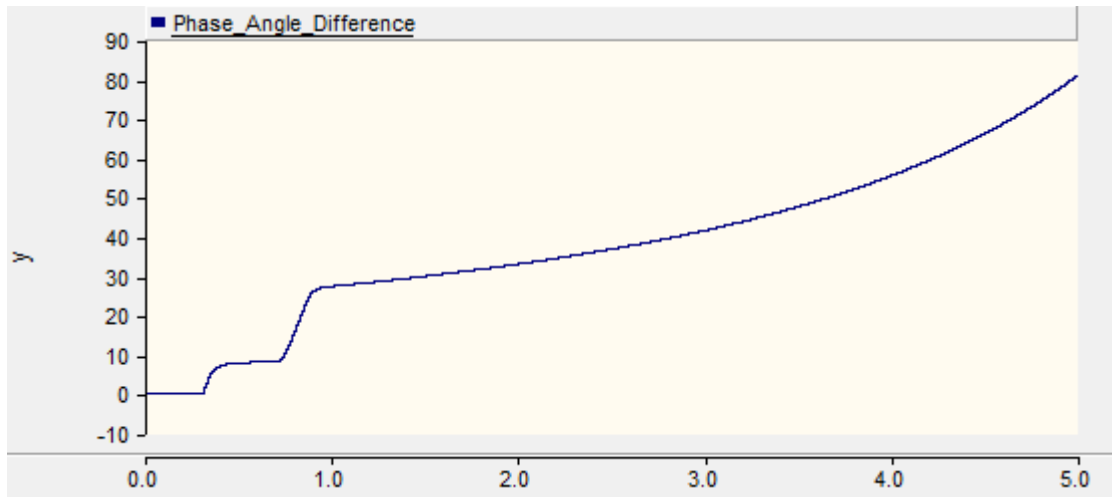


Figure 35. Phase angle difference between VSM1 and VSM2

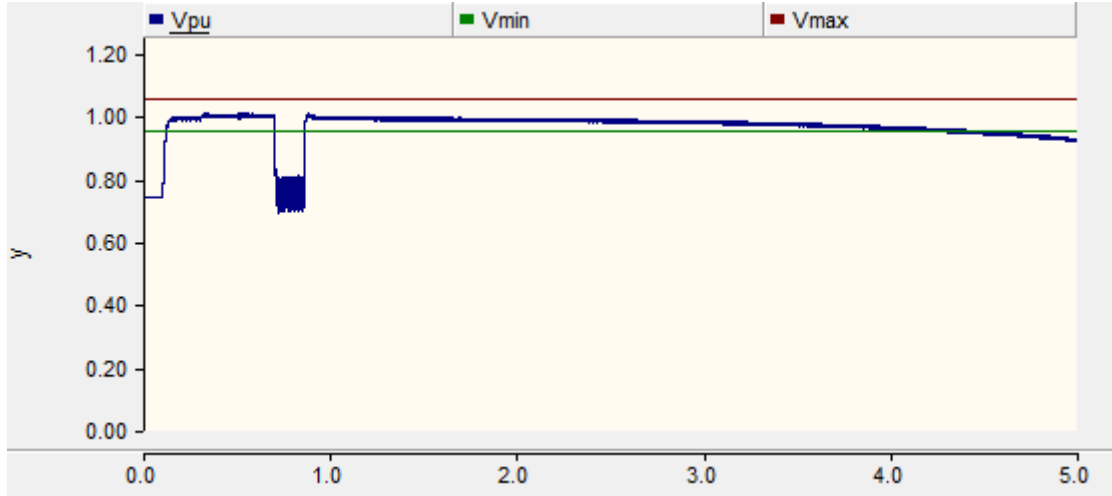


Figure 36. System voltage without phase angle correction algorithm

### 7.5.2 Phase Angle Correction Algorithm Implementation

To address the issue of phase displacement caused by various grid events, a phase correction algorithm will be added to the swing equation. Figure 37 shows the swing equation in control form. Figure 38 shows the modifications to the swing equation that are implemented to correct phase angle error. A PI controller is added to the integration of  $\omega_{VSM}$  to correct error made in the calculation of  $\Theta_{VSM}$ . The  $k_p$  value is held at 0 and the  $k_i$  value is set to 100, so that the phase is gradually corrected to 0 degrees. The input to the PI controller is held at 0 until the phase angle difference reaches 20 degrees, at which point the phase angle error, in radians, is used as the input of the PI controller. Once the phase angle difference is corrected to 0 degrees, the input to the PI controller is again held at 0. This logic is realized using a SR Flip-flop.

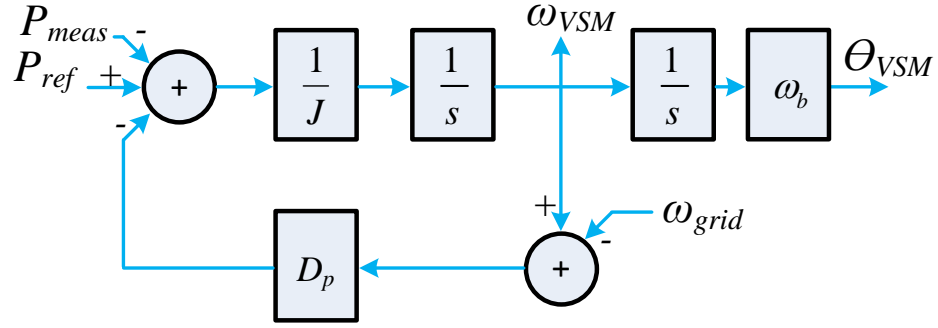


Figure 37. Swing Equation used to calculate  $\omega_{VSM}$  and  $\theta_{VSM}$

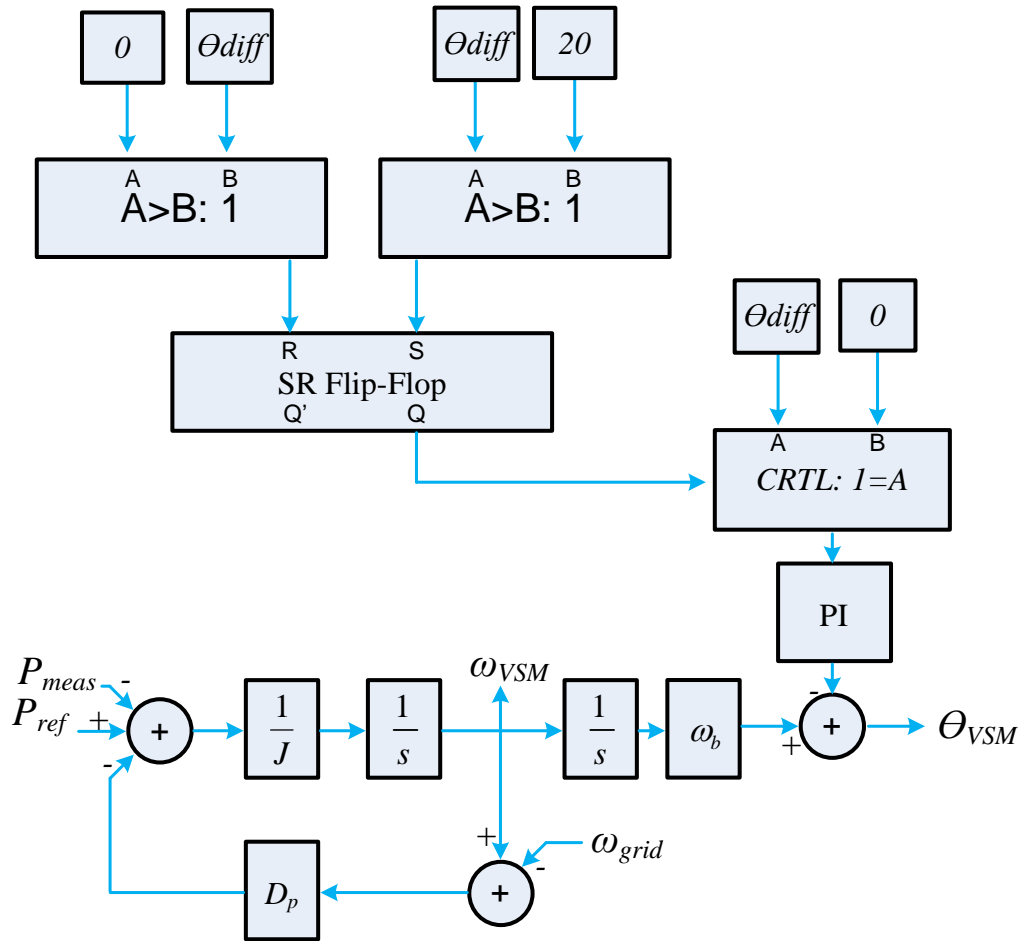


Figure 38. Modified Swing Equation

### 7.5.2.1 Testing Procedure

The same procedure performed in previous sections was used to validate the phase correction algorithm.

### 7.5.2.2 Results

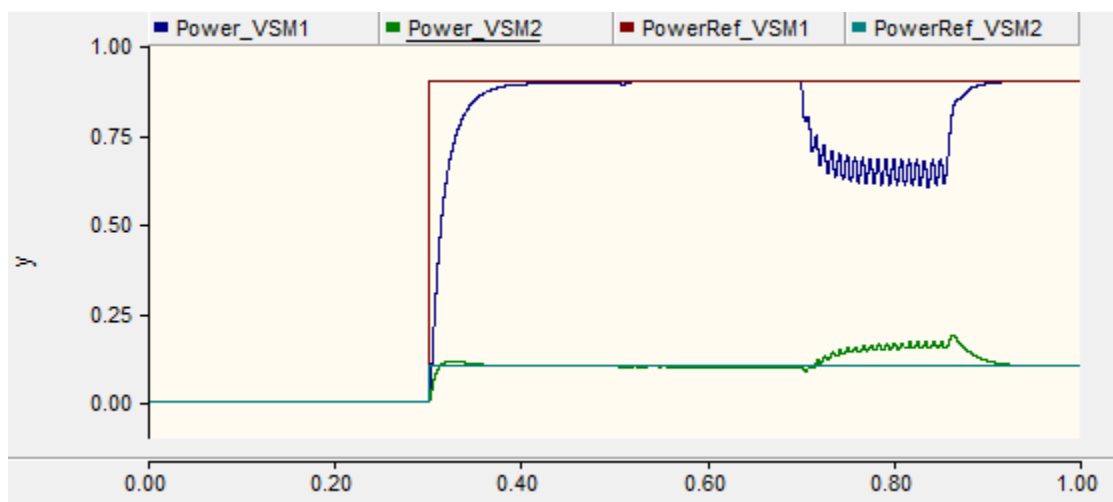


Figure 39. Per unit power output of VSM1 and VSM2

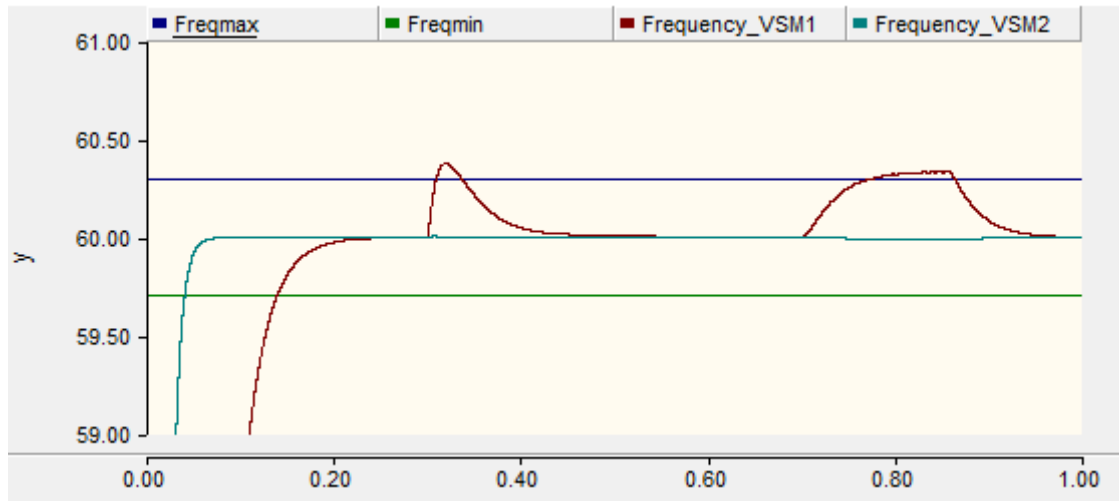


Figure 40. Frequency response of VSM1 and VSM2

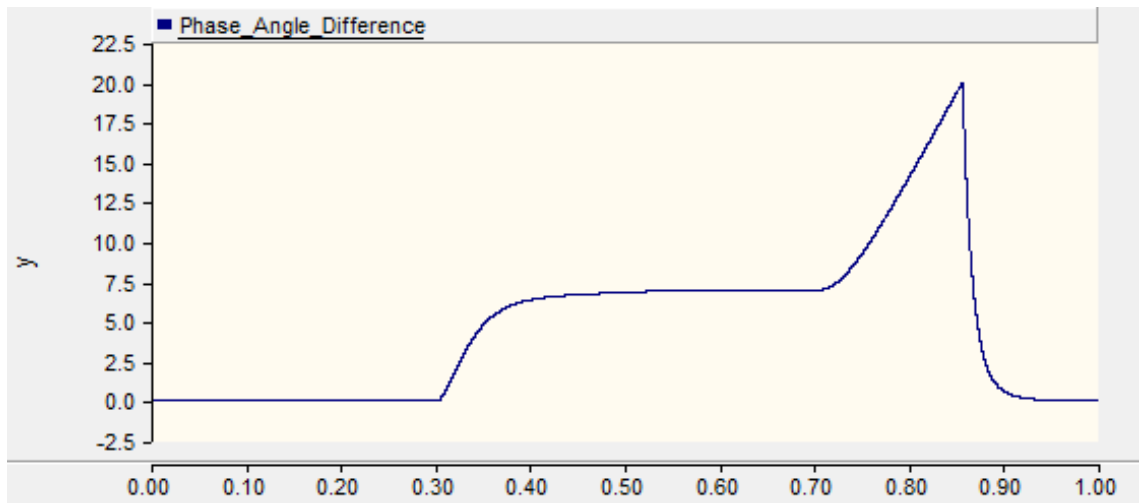


Figure 41. Phase angle difference between VSM1 and VSM2

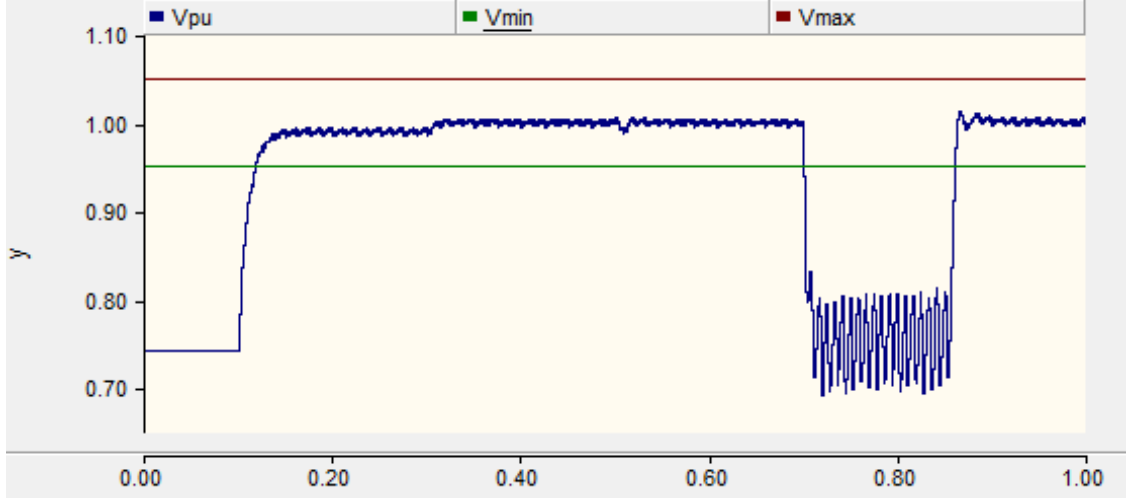


Figure 42. MG load voltage

### 7.5.2.3 Analysis

Again, a power reference increase and fault are applied to the system, as seen in Figure 39. The frequency of the VSMs responded as expected, VSM1 is affected by the grid events while VSM2 holds steady, Figure 40. Therefore, VSM2 stays at its initial phase angle value while the phase angle of VSM1 drifts to 20 degrees during fault recovery. This causes the algorithm to start up and bring the phase angle difference back to 0 degrees, as seen in Figure 41. The proposed algorithm had no ill effects on the system as all three facets of IEEE-1547 synchronization limits, Table 5, do not violate any limits during its correction process. The only recognizable effect is a slight raise in voltage, as seen in Figure 42, but the variation is within the permissible range set according to the limits defined by IEEE-1547.



## **8.0 CONCLUSION**

This work provides insight to the future of MGs and the challenges posed by the change in fuel source. Current VSCs, controlled by conventional PLLs, do not have the inertia needed maintain a steady grid due to the fact that they synchronize to the strongest source, regardless of the quality of said source. The VSM is a promising solution but is not without its flaws.

This work provides a modification to VSM control to eliminate one key flaw, phase angle drift. This problem was identified and solved because large phase angle differences can cause instability in a MG. Over time, grid events will cause VSM's phase angles to change, and potentially depart from the allowable tolerance set by IEEE-1547. If VSMs are to become a regular feature on the grid then VSM DG inverters must synchronize voltage, frequency, and also phase angle in order to provide adequate power quality to customers.

## **8.1 FUTURE WORK**

This work assumed a real load and no line impedance. Adding imaginary impedance, such as inductance and/or capacitance, will mostly increase the need for phase angle correction as power flow angle will become a major issue. This may also affect the results of the algorithm. This researched showed there are no ill effects from implementing a quick phase correction but imaginary impedance may cause power quality issues if the phase angle of a VSC's output is changed rapidly.

## APPENDIX A

### PROOF OF POWER EQUALING TORQUE IN SWING EQUATION

While power and torque can vary depending on the needs of the system, this work shows that even during a severe fault, such a LLG, VSMs have the ability to stay within 0.5 Hz, or 1%, of nominal frequency, 60 Hz. Because VSM frequency stays within 1% of its base value during simulation,  $P=T*\omega$  can be changed to  $P_{pu}=T_{pu}*1=T_{pu}$ . Because power can be approximated as proportional to torque in p.u. the changes made to the swing equation to integrate it to a VSC's controls are valid.

## BIBLIOGRAPHY

- [1] M. I. Henderson, D. Novosel, and M. L. Crow, “Electric Power Grid Modernization Trends, Challenges , and Opportunities,” no. November, 2017.
- [2] H. Kuang, S. Li, and Z. Wu, “Discussion on advantages and disadvantages of distributed generation connected to the grid,” *2011 Int. Conf. Electr. Control Eng. ICECE 2011 - Proc.*, pp. 170–173, 2011.
- [3] R. M. R. Fan, D. Feldman, “U.S. PV Cost Benchmark,” *NREL*, 2017. [Online]. Available: <https://www.nrel.gov/docs/fy17osti/68925.pdf>.
- [4] “U.S. Future Energy Consumption,” *EIA*, 2017. [Online]. Available: <https://www.eia.gov/outlooks/aeo/data/>.
- [5] D. Wang, L. Xiong, and J. Lin, “An inertia emulation method based on improved double-loop control for grid-tied inverters,” *2017 IEEE 3rd Int. Futur. Energy Electron. Conf. ECCE Asia, IFEEC - ECCE Asia 2017*, pp. 2213–2217, 2017.
- [6] N. Ertugrul, “Battery storage technologies, applications and trend in renewable energy,” *2016 IEEE Int. Conf. Sustain. Energy Technol.*, pp. 420–425, 2016.
- [7] A. Hooshyar and R. Iravani, “Microgrid Protection,” *Proc. IEEE*, vol. 105, no. 7, pp. 1332–1353, 2017.
- [8] J. Lee and H. Wang, “Smart Protection Concept for LV Microgrid,” vol. 3, no. March, p. 20, 2010.
- [9] D. T. Ton and M. A. Smith, “The U.S. Department of Energy’s Microgrid Initiative,” *Electr. J.*, vol. 25, no. 8, pp. 84–94, 2012.
- [10] S. Golestan, J. M. Guerrero, and J. C. Vasquez, “Three-Phase PLLs: A Review of Recent Advances,” *IEEE Trans. Power Electron.*, vol. 32, no. 3, pp. 1897–1907, 2017.
- [11] M. Surprenant, I. Hiskens, and G. Venkataramanan, “Phase locked loop control of inverters in a microgrid,” *2011 IEEE Energy Convers. Congr. Expo.*, pp. 667–672, 2011.
- [12] M. A. Anuradha and A. Massoud, *IEEE Vision for Smart Grid Controls: 2030 and Beyond*. 2013.
- [13] G. Joos, J. Reilly, W. Bower, and R. Neal, “The Need for Standardization: The Benefits to the Core Functions of the Microgrid Control System,” *IEEE Power Energy Mag.*, vol. 15, no. 4, pp. 32–40, 2017.
- [14] D. E. Olivares *et al.*, “Trends in microgrid control,” *IEEE Trans. Smart Grid*, vol. 5, no. 4, pp. 1905–1919, 2014.

- [15] “IEEE Guide for Design , Operation , and Integration of Distributed Resource Island Systems with Electric Power Systems IEEE Standards Coordinating Committee 21 Sponsored by the,” 2011.
- [16] J. A. P. Lopes, C. L. Moreira, and A. G. Madureira, “Defining control strategies for microgrids islanded operation,” *IEEE Trans. Power Syst.*, vol. 21, no. 2, pp. 916–924, 2006.
- [17] F. D’Agostino, S. Massucco, F. Silvestro, A. Fidigatti, F. Monachesi, and E. Ragaini, “Low voltage microgrid islanding through adaptive load shedding,” *Conf. Proc. - 2017 17th IEEE Int. Conf. Environ. Electr. Eng. 2017 1st IEEE Ind. Commer. Power Syst. Eur. IEEEIC / I CPS Eur. 2017*, 2017.
- [18] T. John and S. Ping Lam, “Voltage and frequency control during microgrid islanding in a multi-area multi-microgrid system,” *IET Gener. Transm. Distrib.*, vol. 11, no. 6, pp. 1502–1512, 2017.
- [19] M. Patil, S. R. Bhide, and S. S. Bhat, “Experimenting with IEC 61850 and GOOSE messaging,” *ICPCES*, pp. 1–6, 2017.
- [20] Q. C. Zhong and G. Weiss, “Synchronverters: Inverters that mimic synchronous generators,” *IEEE Trans. Ind. Electron.*, vol. 58, no. 4, pp. 1259–1267, 2011.
- [21] S. D’Arco and J. A. Suul, “A synchronization controller for grid reconnection of islanded virtual synchronous machines,” *2015 IEEE 6th Int. Symp. Power Electron. Distrib. Gener. Syst. PEDG 2015*, 2015.
- [22] S. Y. Caliskan and P. Tabuada, “Uses and abuses of the swing equation model,” *Proc. IEEE Conf. Decis. Control*, vol. 54rd IEEE, no. Cdc, pp. 6662–6667, 2015.
- [23] M. Rahimian and K. Butler-Purry, “Modeling of synchronous machines with damper windings for condition monitoring,” *2009 IEEE Int. Electr. Mach. Drives Conf. IEMDC ’09*, pp. 577–584, 2009.
- [24] “IEEE Standard for Interconnecting Distributed Resources with Electric Power Systems Standards,” 2004.